

Special points for hybrid neutron stars in the mass-radius diagram

David Blaschke^{a,b,c} & Mateusz Cierniak^a

a – University Wrocław, b - JINR Dubna, c – NRNU (MEPhI) Moscow

0. Introduction: Recent relevant multi-messenger observations
1. The special point and its properties
2. New paradigm: Only hybrid stars fulfill new M-R constraints
3. Outlook: Supernovae & Mergers in the QCD phase diagram

6th Int. Conf. Modern Physics of Compact Stars, Yerevan, 30.09.2021



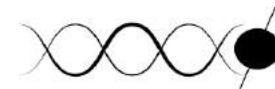
Grant No. UMO 2019 / 33 / B / ST9 / 03059



Grant No. 17-12-01427



Grant No. 18-02-40137



PHAROS
THE MULTI-MESSENGER
PHYSICS AND ASTROPHYSICS
OF NEUTRON STARS



NICER radius measurement on PSR J0740+6620

New, large NICER radius for J0740: Riley et al., 2105.06980; Miller et al., 2105.06979

Attention:

Above $\sim 1.5 M_{\text{sun}}$ hyperons
Appear in the center of neutron stars.

Non-hyperonic nuclear EoS (APR)
Are no longer applicable for
High-mass neutron stars $\sim 2M_{\text{sun}}$!

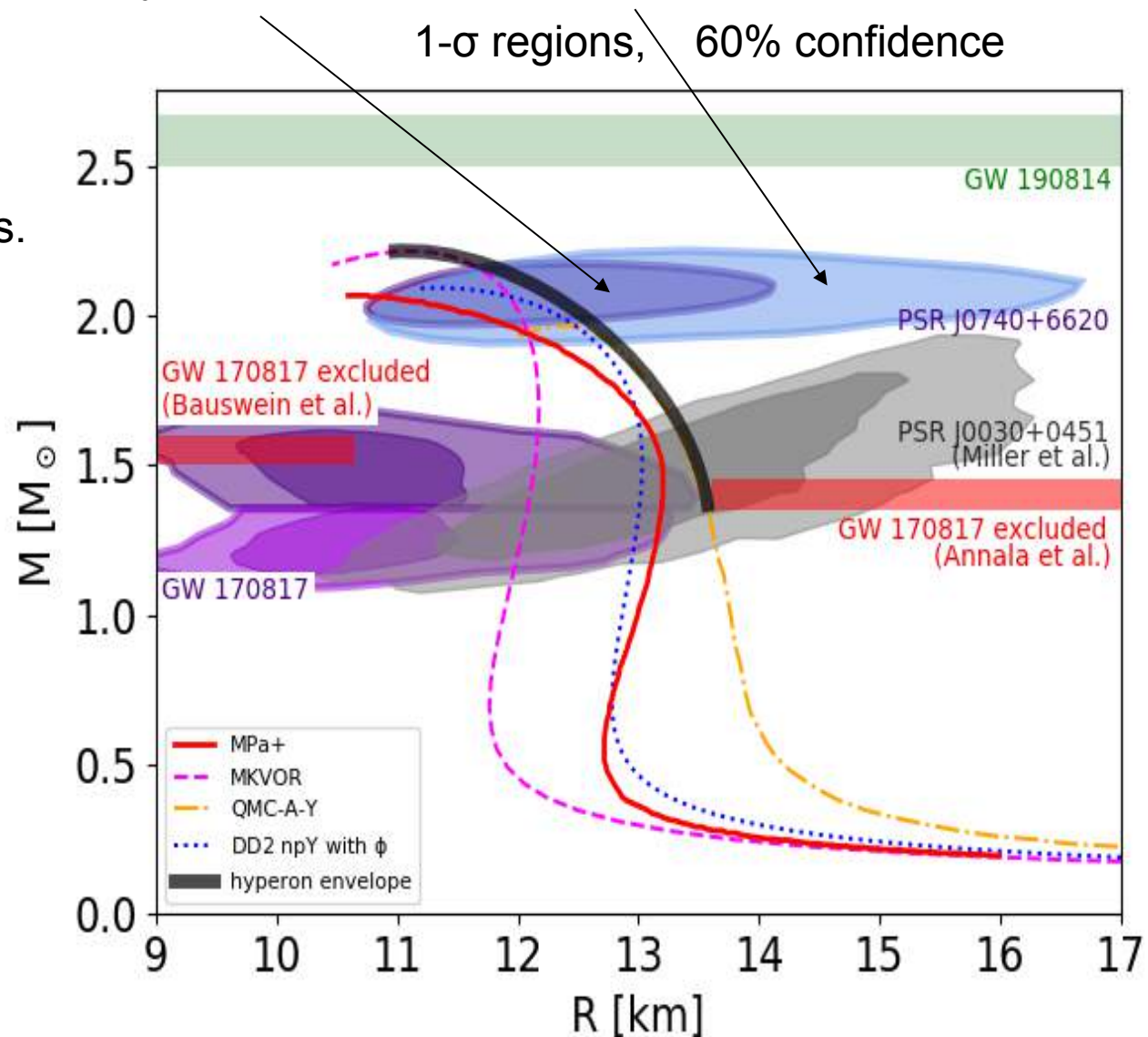
Microscopic EoS need high-density
Stiffening of the hypernuclear EoS,
e.g., by multi-pomeron interactions.

Yamamoto et al., PRC 96 (2017)

Relativistic mean-field EoS have a
Maximal NS radius $R_{2.0} \sim 13$ km

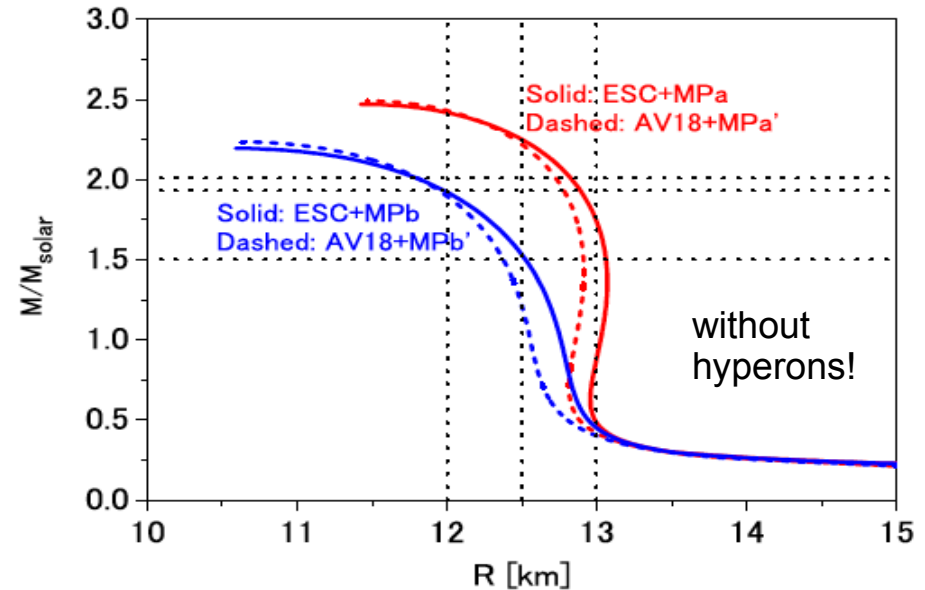
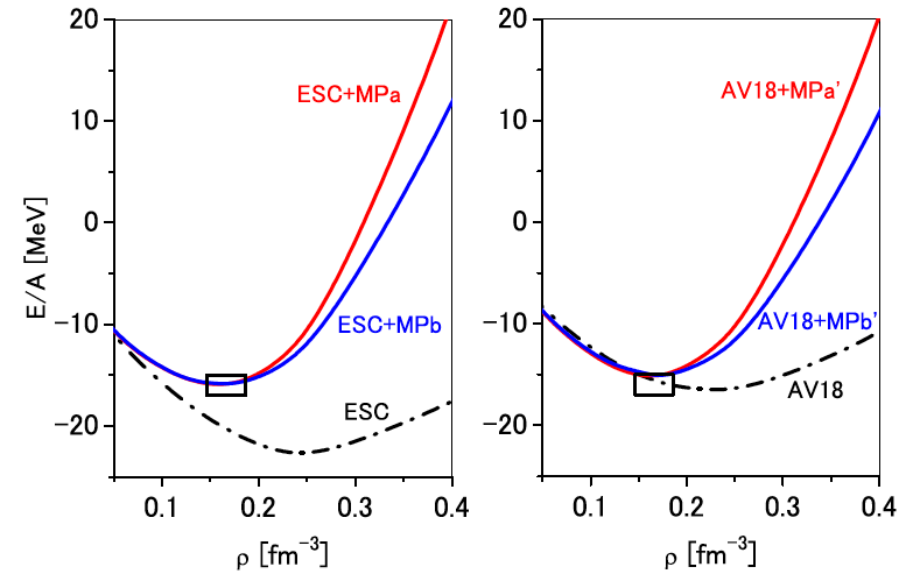
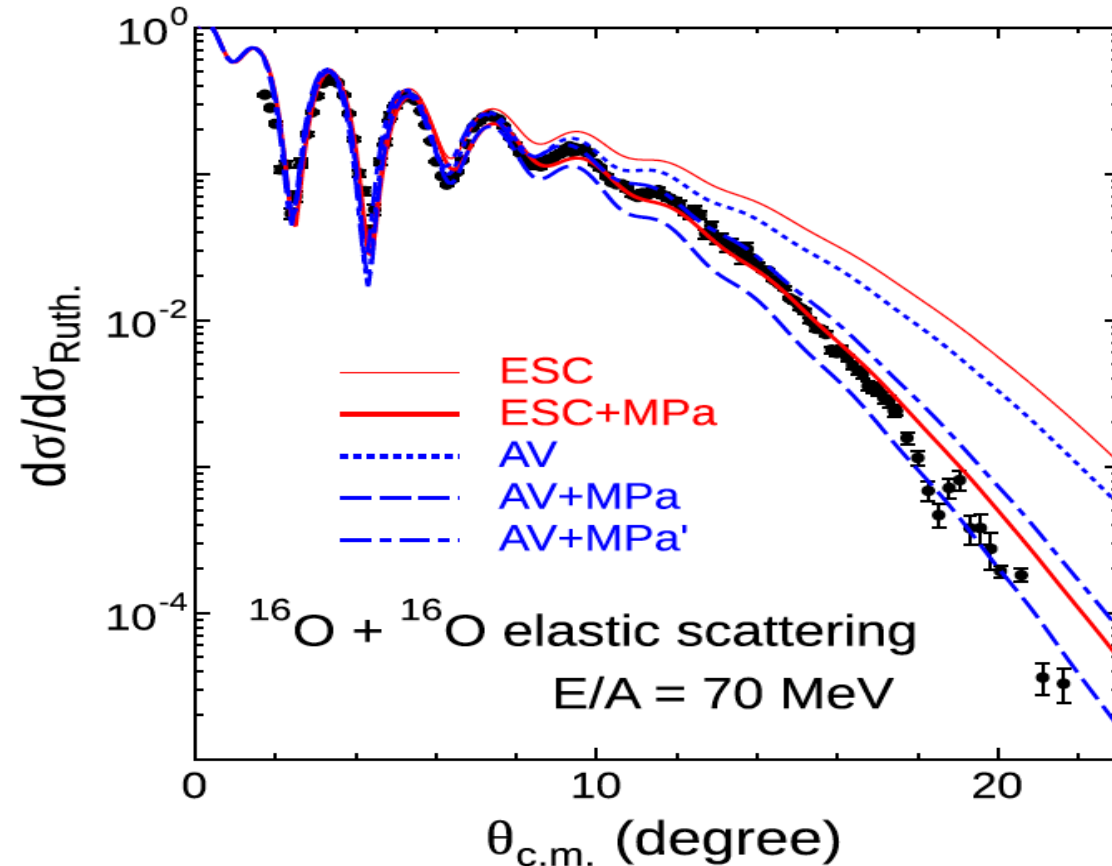
Way out:

early deconfinement to color
superconducting, stiff quark matter !



Shall the APR EoS be abandoned?

Y. Yamamoto, H. Togashi, T. Tamagawa, T. Furumoto, N. Yasutake, T. Rijken, PRC 96 (2017)



Short-range multipomeron exchange potential (MPP) added to AV18 potential gives significant improvement of large-angle scattering cross section (s.a.) and the Nuclear saturation properties, when compared to APR.
 → Neutron star radii $R(M < 2 M_{\text{sun}}) > 12 \text{ km} !!$

What is the special point? What are its properties?

The TOV equation

$$\frac{\partial P(r)}{\partial r} = - \frac{\epsilon(r)M(r) \left(1 + \frac{P(r)}{\epsilon(r)}\right) \left(1 + \frac{4\pi r^3 P(r)}{M(r)}\right)}{r^2 \left(1 - \frac{2M(r)}{r}\right)}, \quad \frac{\partial M(r)}{\partial r} = 4\pi r^2 \epsilon(r).$$

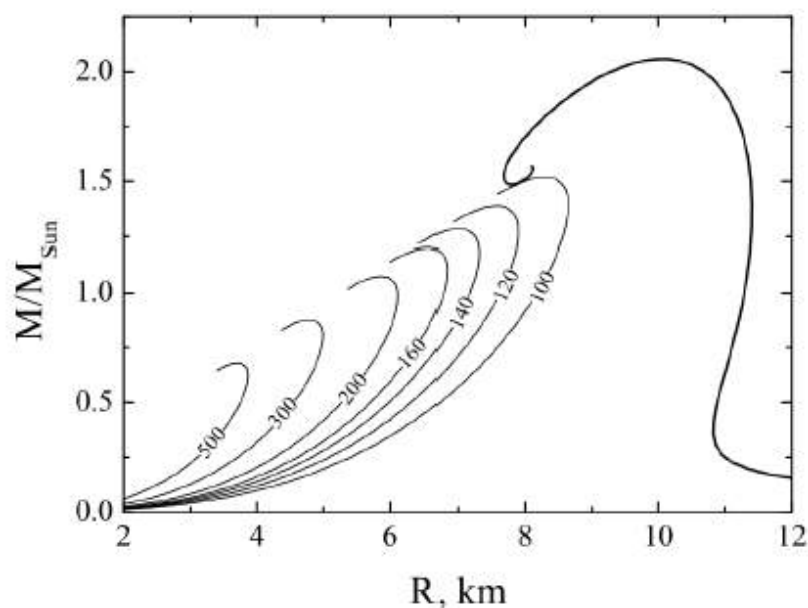


Fig. 1. Mass-radius diagram for a star made of ordinary matter (thick line) and purely quark stars (thin lines). The numbers at the lines indicate the parameter B .

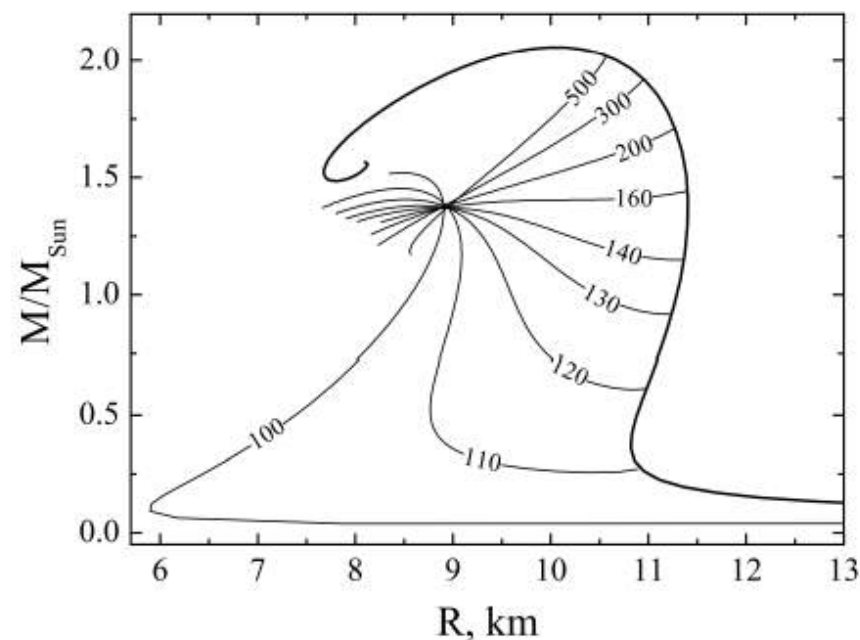


Fig. 2. Mass-radius diagram of hybrid stars for various values of the parameter B

What is the special point? What are its properties?

The constant-speed-of-sound (CSS) model:

– dimensionless baryochemical potential

$$\hat{\mu}_B = \frac{\mu_B}{\mu_{scale}} = \left(\frac{p+B}{A} \right)^{1/(1+\beta)},$$

– pressure

$$p(\mu_B) = A\hat{\mu}_B^{1+\beta} - B,$$

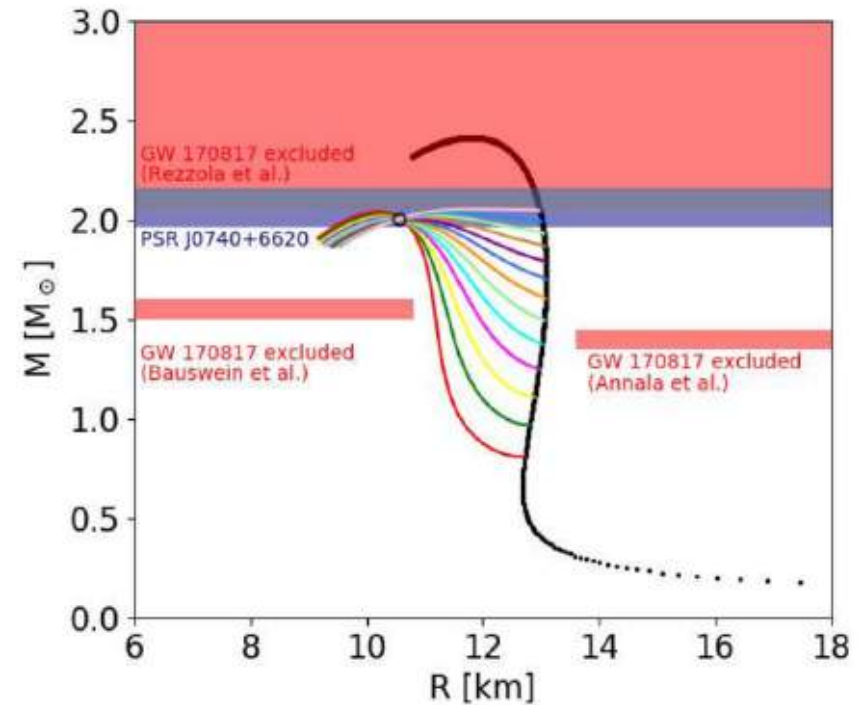
– baryon density

$$n_B(\mu_B) = (1 + \beta) \frac{A}{\mu_{scale}} \hat{\mu}_B^\beta,$$

– energy density

$$\epsilon = B + \beta A \hat{\mu}_B^{1+\beta},$$

– $p(\epsilon)$ relation: $\epsilon = \beta p + (1 + \beta)B$.



What is the special point? What are its properties?

The constant-speed-of-sound (CSS) model:

- dimensionless baryochemical potential

$$\hat{\mu}_B = \frac{\mu_B}{\mu_{scale}} = \left(\frac{p+B}{A} \right)^{1/(1+\beta)},$$

- pressure

$$p(\mu_B) = A\hat{\mu}_B^{1+\beta} - B,$$

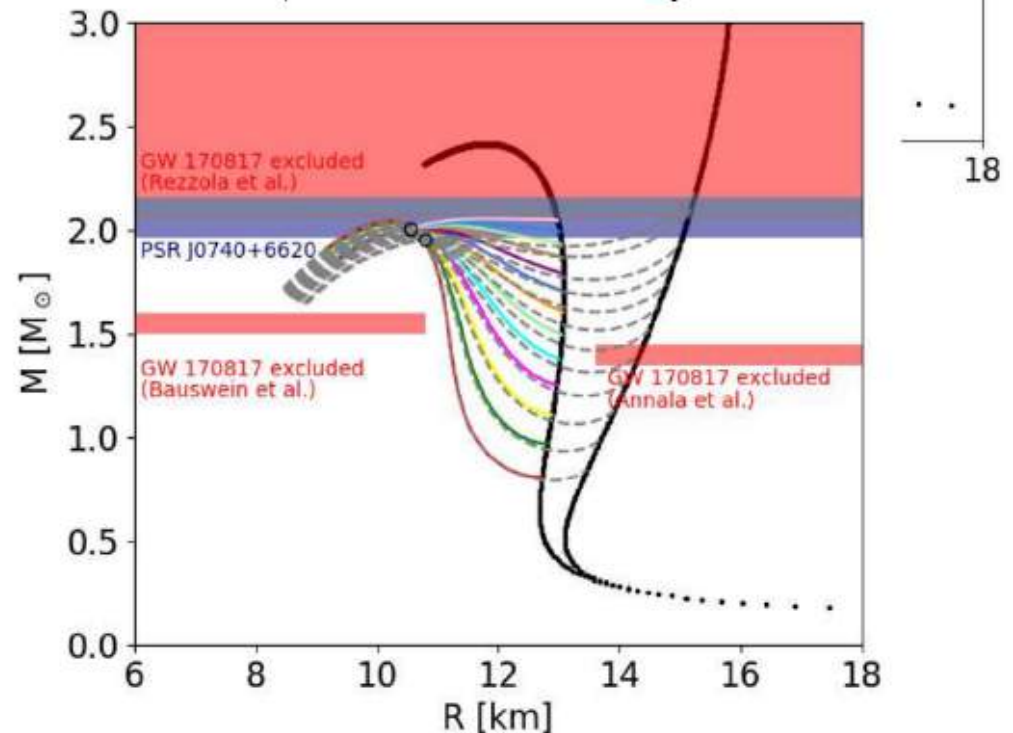
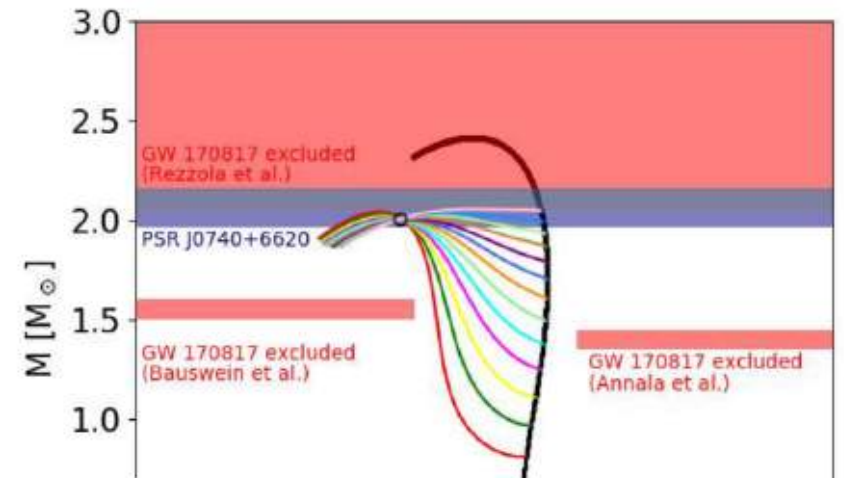
- baryon density

$$n_B(\mu_B) = (1 + \beta) \frac{A}{\mu_{scale}} \hat{\mu}_B^\beta,$$

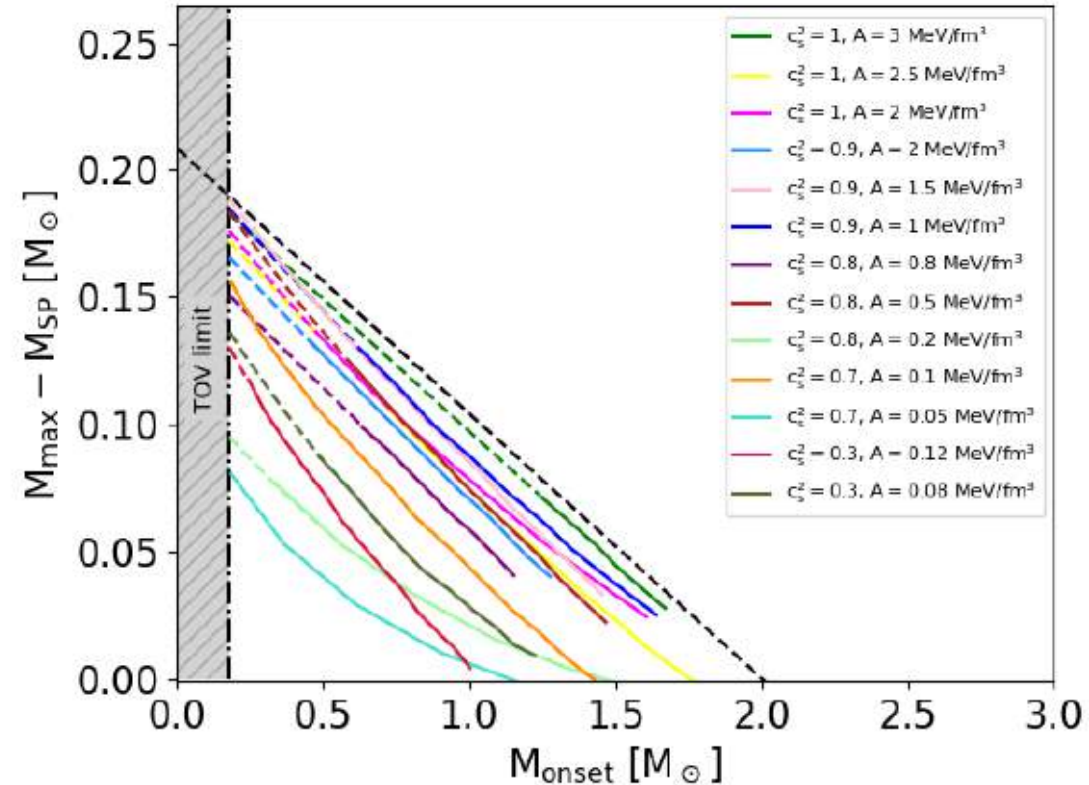
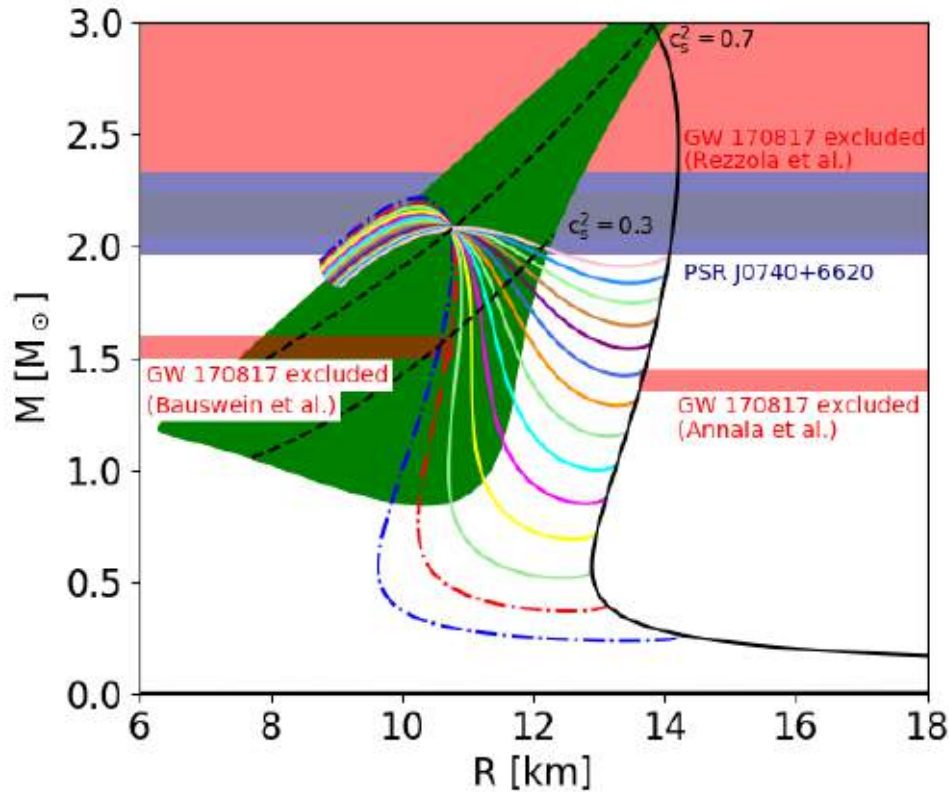
- energy density

$$\epsilon = B + \beta A \hat{\mu}_B^{1+\beta},$$

- $p(\epsilon)$ relation: $\epsilon = \beta p + (1 + \beta)B$.

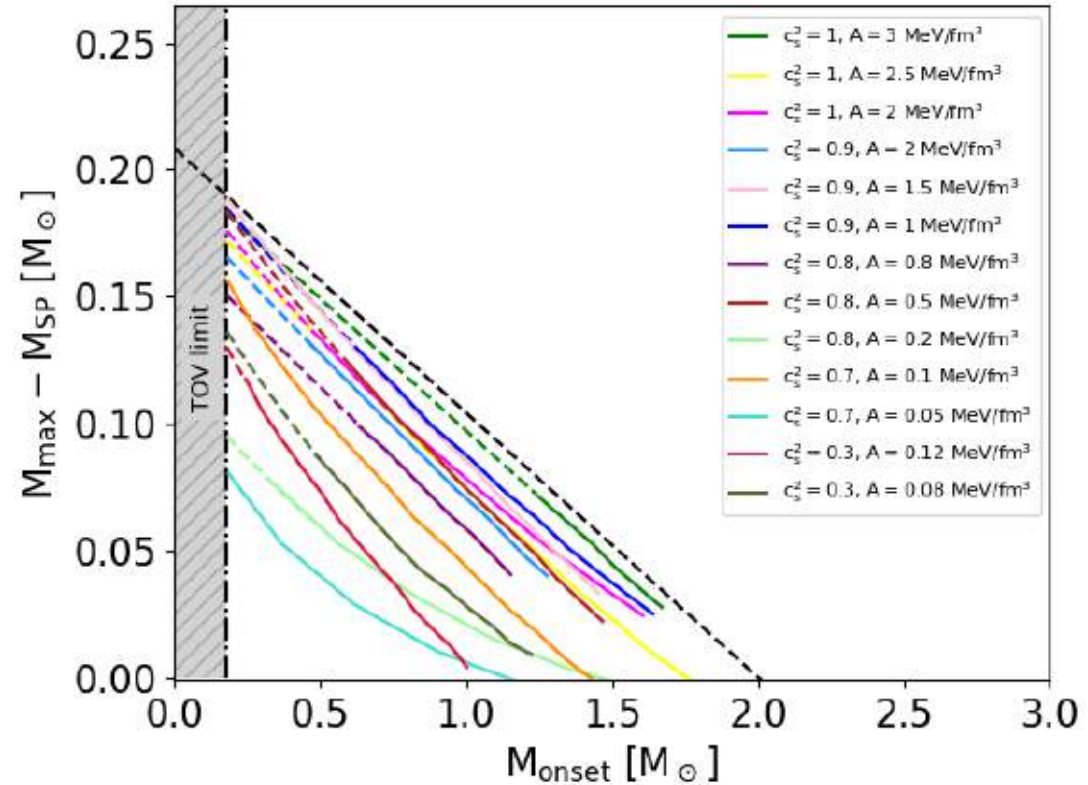
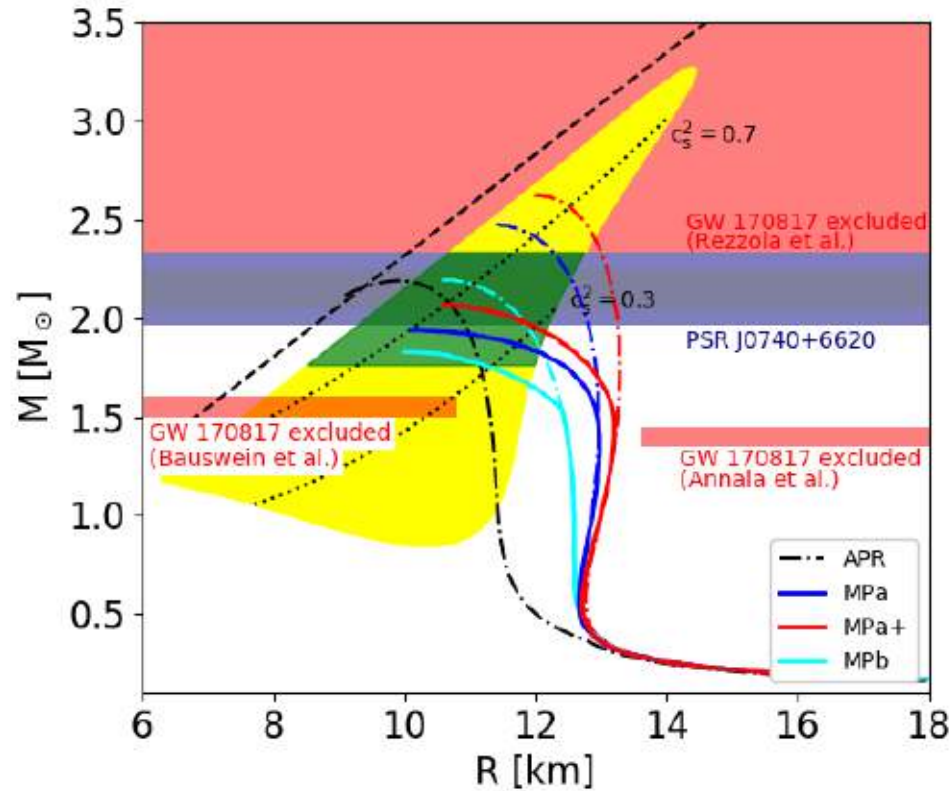


What is the special point? What are its properties?



$$M_{max} = M_{SP} + 0.208M_{\odot} - 0.104M_{onset}$$

What is the special point? What are its properties?



$$M_{max} = M_{SP} + 0.208M_{\odot} - 0.104M_{onset}$$

Dependence on the phase transition construction?

The mixed phase parabolic ansatz:

$$P_M(\mu) = \alpha_2(\mu - \mu_c)^2 + \alpha_1(\mu - \mu_c) + (1 + \Delta_p)P_c,$$

Gibbs condition for phase equilibrium:

$$\begin{aligned} P_H(\mu_H) &= P_M(\mu_H), \\ P_Q(\mu_Q) &= P_M(\mu_Q), \\ \frac{\partial^k}{\partial \mu^k} P_H(\mu_H) &= \frac{\partial^k}{\partial \mu^k} P_M(\mu_H), \\ \frac{\partial^k}{\partial \mu^k} P_Q(\mu_Q) &= \frac{\partial^k}{\partial \mu^k} P_M(\mu_Q). \end{aligned}$$

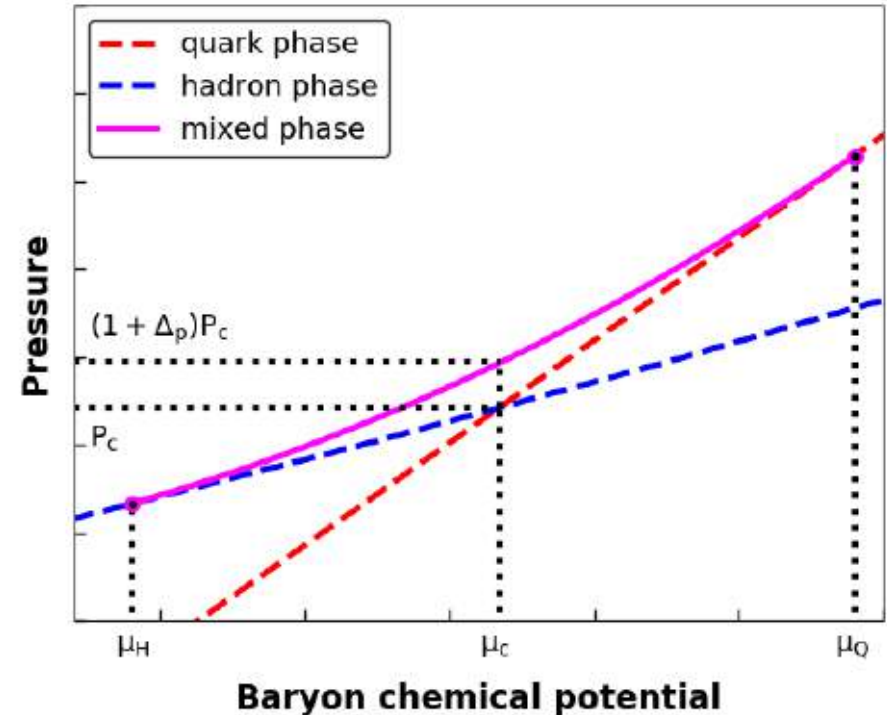
Derived parameters ($k = 1$):

$$\alpha_1 = \frac{-2\kappa_1 + \kappa_2(\mu_c - \mu_H)}{2(\mu_c - \mu_Q)(\mu_H - \mu_Q)},$$

$$\alpha_2 = \frac{-2\kappa_1 + \kappa_2(\mu_c - \mu_Q)}{2(\mu_c - \mu_H)(\mu_H - \mu_Q)},$$

$$\kappa_1 = n_Q(\mu_c - \mu_Q) - n_H(\mu_c - \mu_H) + P_Q - P_H,$$

$$\kappa_2 = n_Q - n_H.$$



Dependence on the phase transition construction?

The mixed phase parabolic ansatz:

$$P_M(\mu) = \alpha_2(\mu - \mu_c)^2 + \alpha_1(\mu - \mu_c) + (1 + \Delta_p)P_c,$$

Gibbs condition for phase equilibrium:

$$P_H(\mu_H) = P_M(\mu_H),$$

$$P_Q(\mu_Q) = P_M(\mu_Q),$$

$$\frac{\partial^k}{\partial \mu^k} P_H(\mu_H) = \frac{\partial^k}{\partial \mu^k} P_M(\mu_H),$$

$$\frac{\partial^k}{\partial \mu^k} P_Q(\mu_Q) = \frac{\partial^k}{\partial \mu^k} P_M(\mu_Q).$$

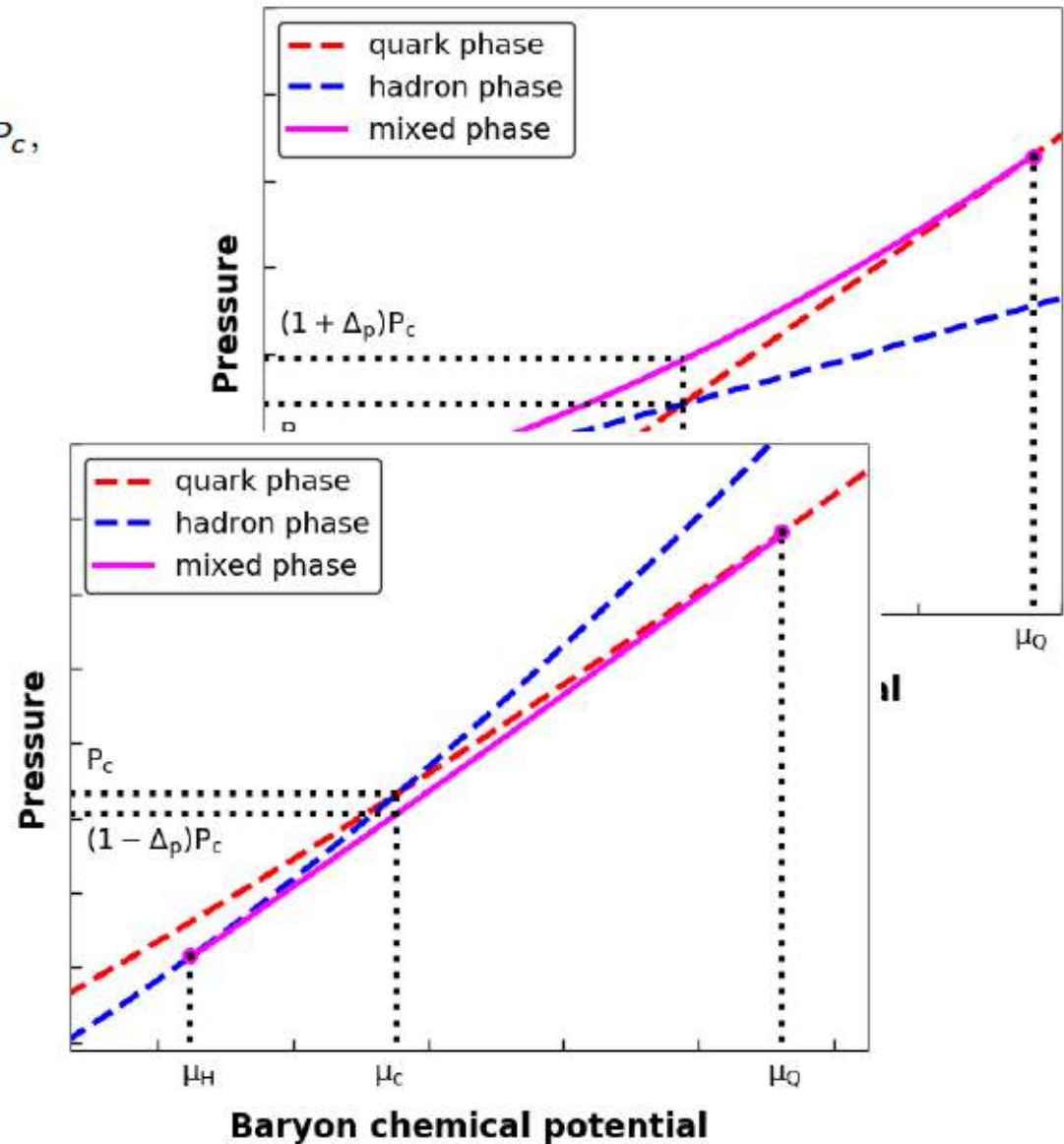
Derived parameters ($k = 1$):

$$\alpha_1 = \frac{-2\kappa_1 + \kappa_2(\mu_c - \mu_H)}{2(\mu_c - \mu_Q)(\mu_H - \mu_Q)},$$

$$\alpha_2 = \frac{-2\kappa_1 + \kappa_2(\mu_c - \mu_Q)}{2(\mu_c - \mu_H)(\mu_H - \mu_Q)},$$

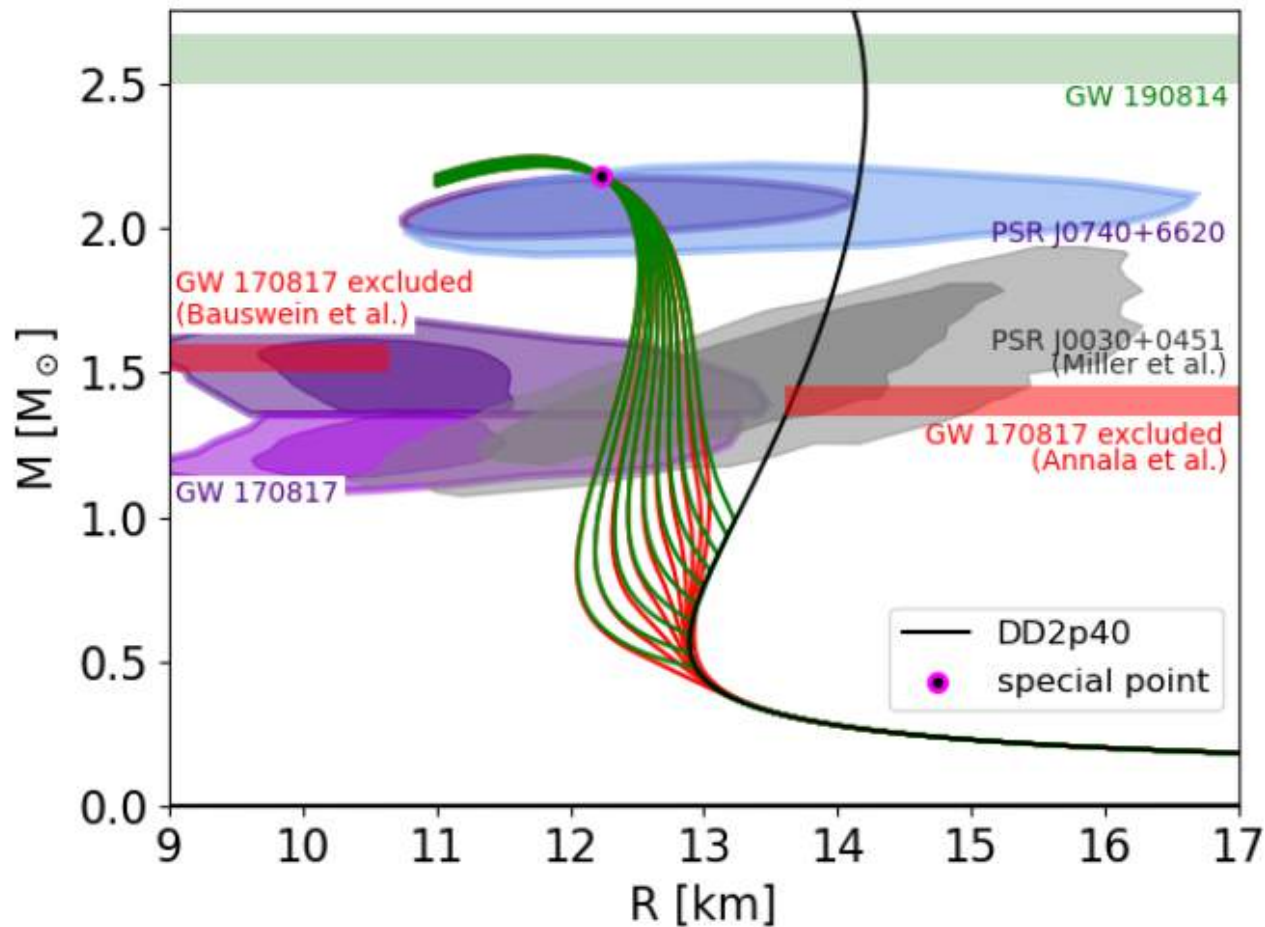
$$\kappa_1 = n_Q(\mu_c - \mu_Q) - n_H(\mu_c - \mu_H) + P_Q - P_H,$$

$$\kappa_2 = n_Q - n_H.$$



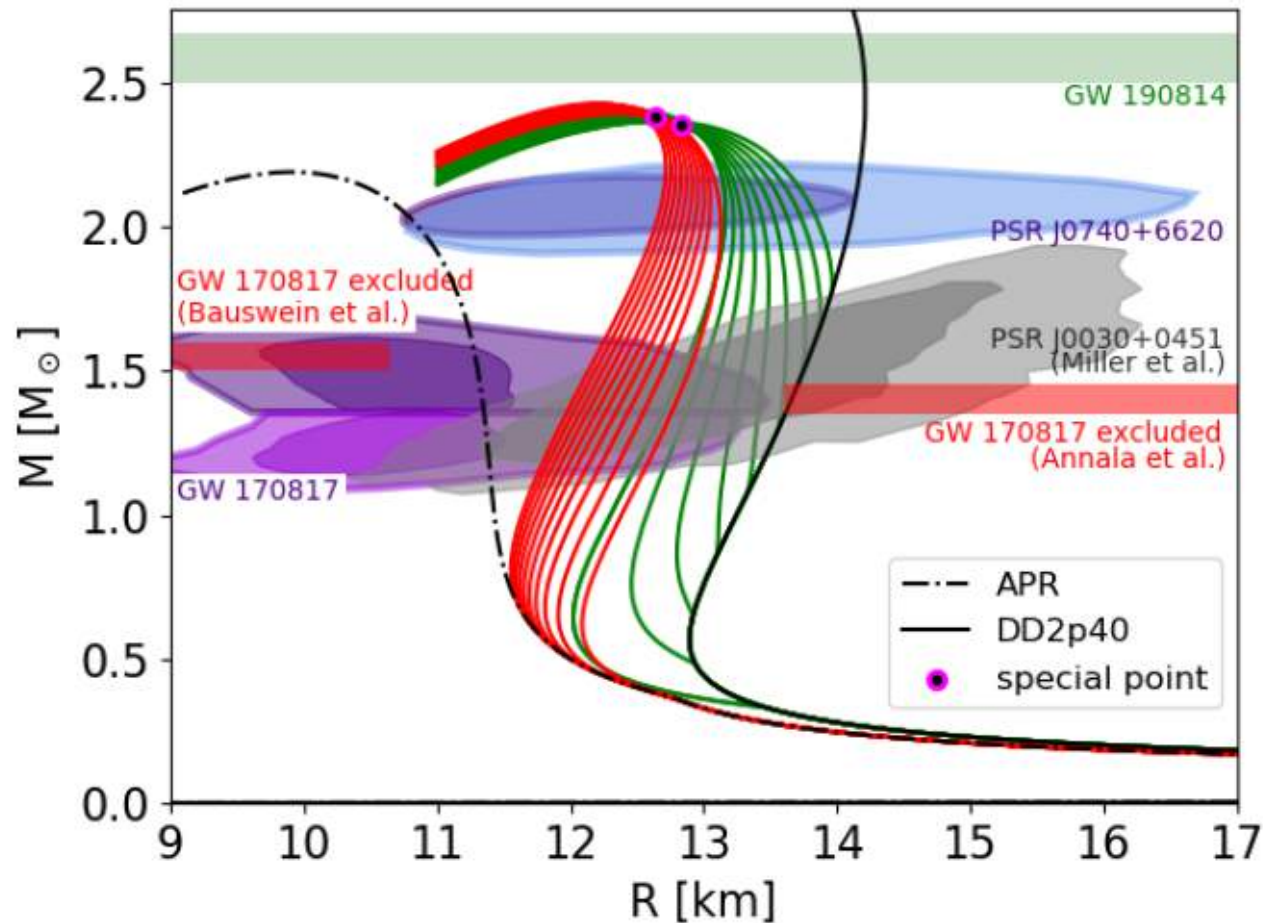
Dependence on the phase transition construction?

Invariance w.r.t. Maxwell \rightarrow mixed phase construction (pasta phases)



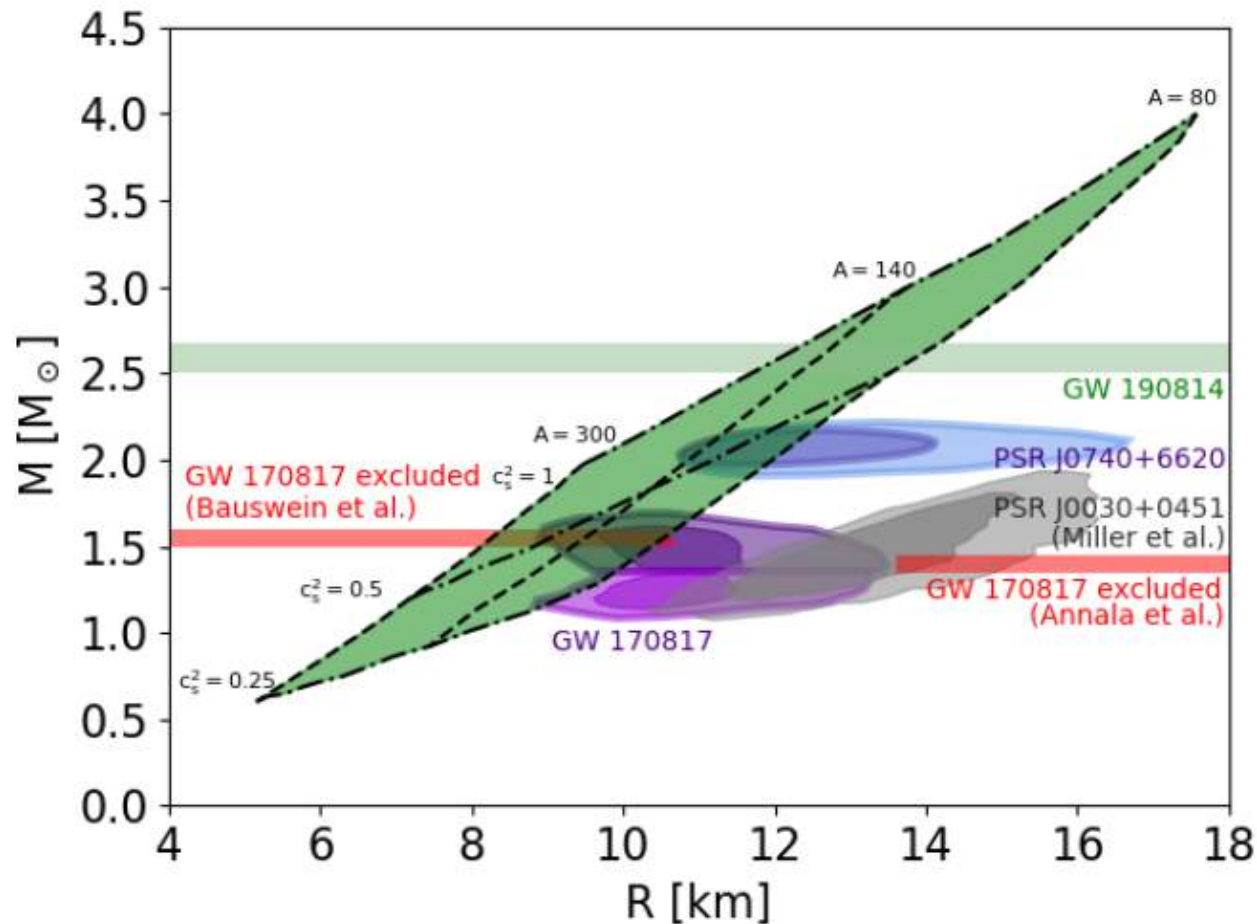
Dependence on the phase transition construction?

Invariance w.r.t. Maxwell \rightarrow interpolation construction (soft - stiff transition)



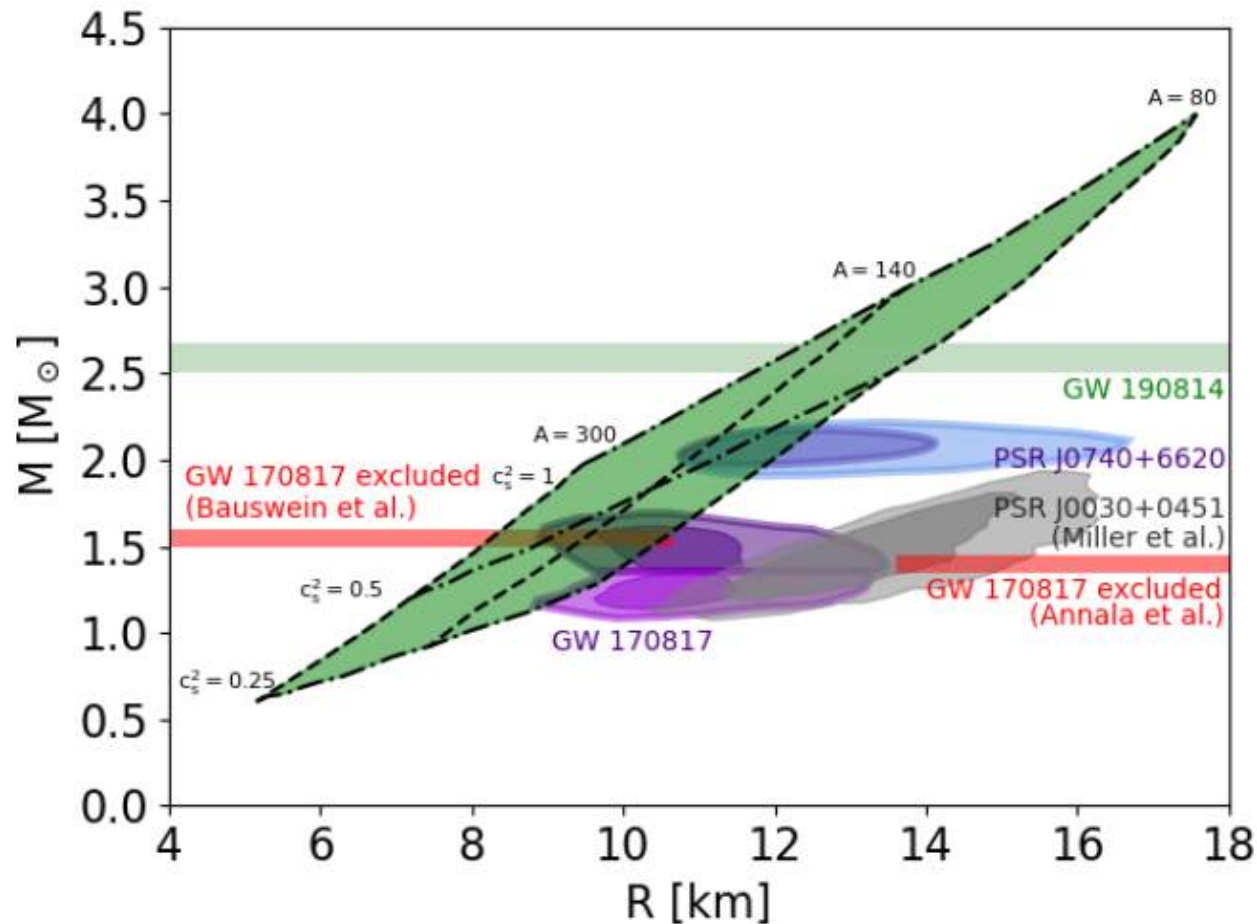
Mapping the special point locations ...

Special point locations for constant sound speed c_s

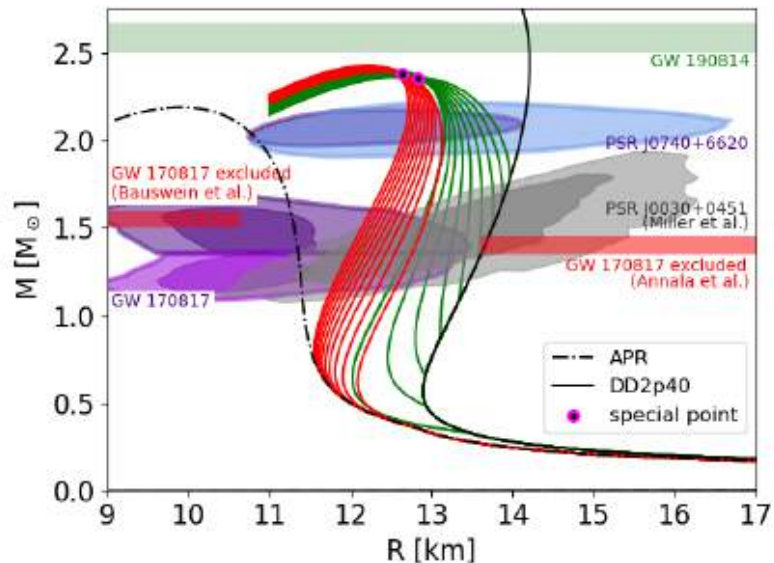
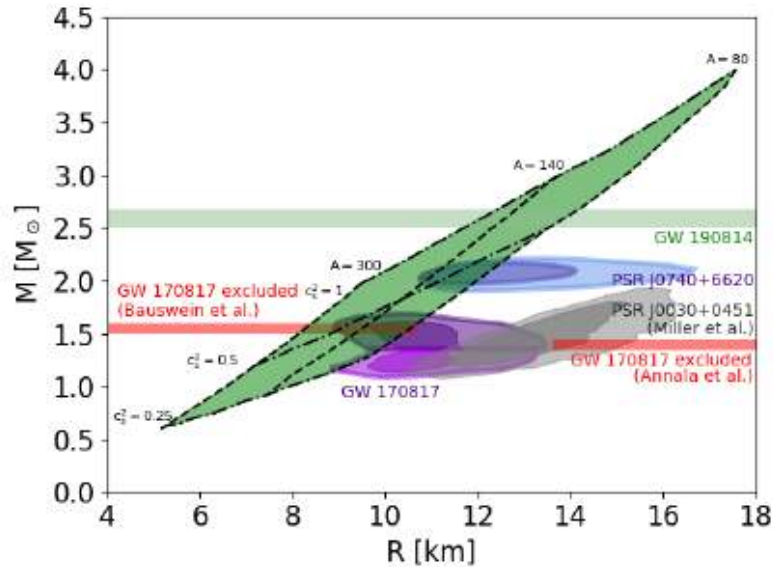


Mapping the special point locations ...

Special point locations for constant sound speed c_s
... and constant prefactor A



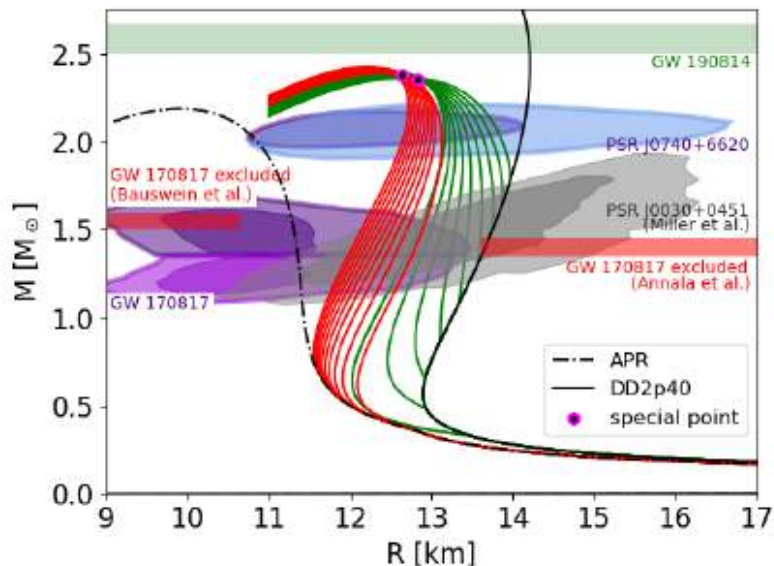
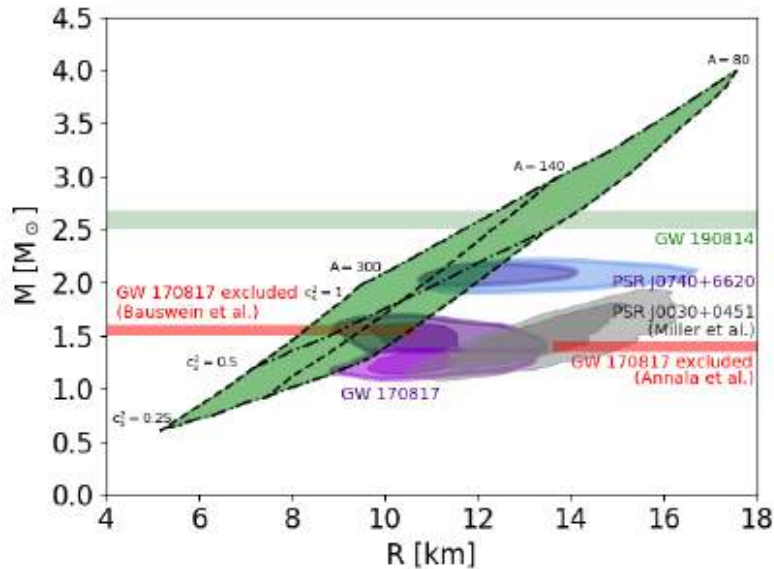
Mapping the special point locations ...



| c_s^2 | M_{SP} [M_\odot] | R_{min} [km] | R_{max} [km] |
|---------|---------------------------|-------------------|-------------------|
| 0.35 | 1.82 | - | - |
| 0.40 | 2.07 | 12.18 | 12.29 |
| 0.45 | 2.30 | 11.84 | 13.41 |
| 0.50 | 2.50 | 11.56 | 13.91 |
| 0.55 | 2.68 | 11.30 | 14.20 |
| 0.60 | 2.86 | 11.05 | 14.45 |
| 0.70 | 3.22 | 10.67 | 14.67 |
| 1.00 | 4.00 | 9.95 | 14.84 |

The values of c_s^2 , largest possible M_{SP} and the radii range ($R_{min} - R_{max}$) of a $2 M_\odot$ hybrid star.

Mapping the special point locations ...



| c_s^2 | M_{SP} [M_\odot] | R_{min} [km] | R_{max} [km] |
|-------------|---------------------------|-------------------|-------------------|
| 0.35 | 1.82 | - | - |
| 0.40 | 2.07 | 12.18 | 12.29 |
| 0.45 | 2.30 | 11.84 | 13.41 |
| 0.50 | 2.50 | 11.56 | 13.91 |
| 0.55 | 2.68 | 11.30 | 14.20 |
| 0.60 | 2.86 | 11.05 | 14.45 |
| 0.70 | 3.22 | 10.67 | 14.67 |
| 1.00 | 4.00 | 9.95 | 14.84 |

The values of c_s^2 , largest possible M_{SP} and the radii range ($R_{min} - R_{max}$) of a $2 M_\odot$ hybrid star. **Bold red rows correspond to the nINJL fit from [6].**

Constant sound speed (CSS) vs. nonlocal NJL model

$$\mathcal{L} = \bar{\psi} (-i\not{\partial} + m_c) \psi - \frac{G_S}{2} j_S^f j_S^f - \frac{G_D}{2} [j_D^a]^\dagger j_D^a + \frac{G_V}{2} j_V^\mu j_V^\mu, \quad \eta_D = G_D/G_S \text{ and } \eta_V = G_V/G_S$$

Nonlocal currents, formfactor $g(z)$

$$j_S^f(x) = \int d^4 z g(z) \bar{\psi}(x + \frac{z}{2}) \Gamma^f \psi(x - \frac{z}{2}),$$

$$j_D^a(x) = \int d^4 z g(z) \bar{\psi}_C(x + \frac{z}{2}) i\gamma_5 \tau_2 \lambda^a \psi(x - \frac{z}{2}),$$

$$j_V^\mu(x) = \int d^4 z g(z) \bar{\psi}(x + \frac{z}{2}) i\gamma_\mu \psi(x - \frac{z}{2}),$$

CSS equation of state

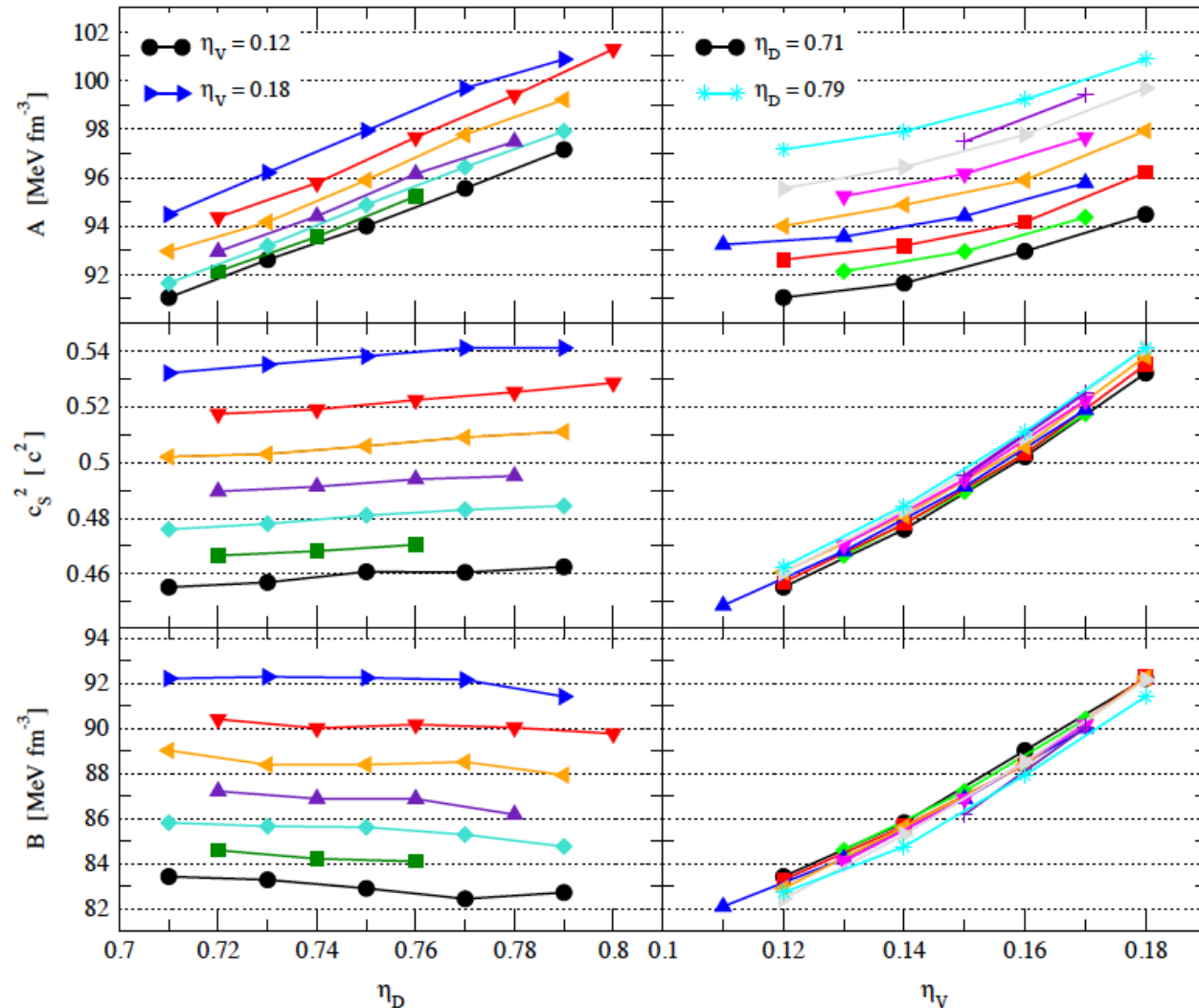
$$P(\mu) = A \left(\frac{\mu}{\mu_x} \right)^{1+\beta} - B,$$

Fitted relationship, see figure \rightarrow

$$A = a_1 \eta_D + b_1 \eta_V^2 + c_1$$

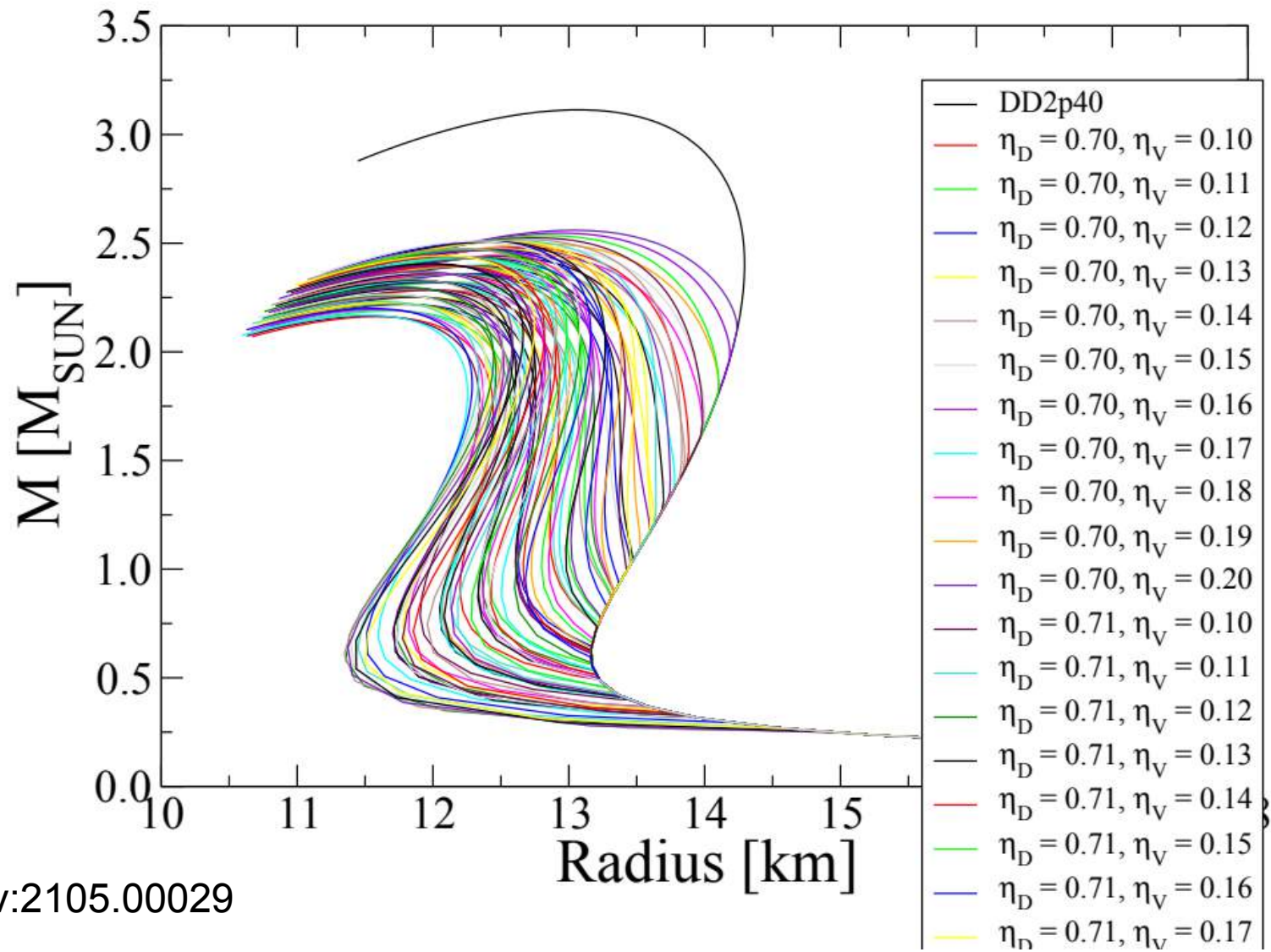
$$c_s^2 = a_2 \eta_D + b_2 \eta_V^2 + c_2$$

$$B = a_3 \eta_D + b_3 \eta_V^2 + c_3,$$



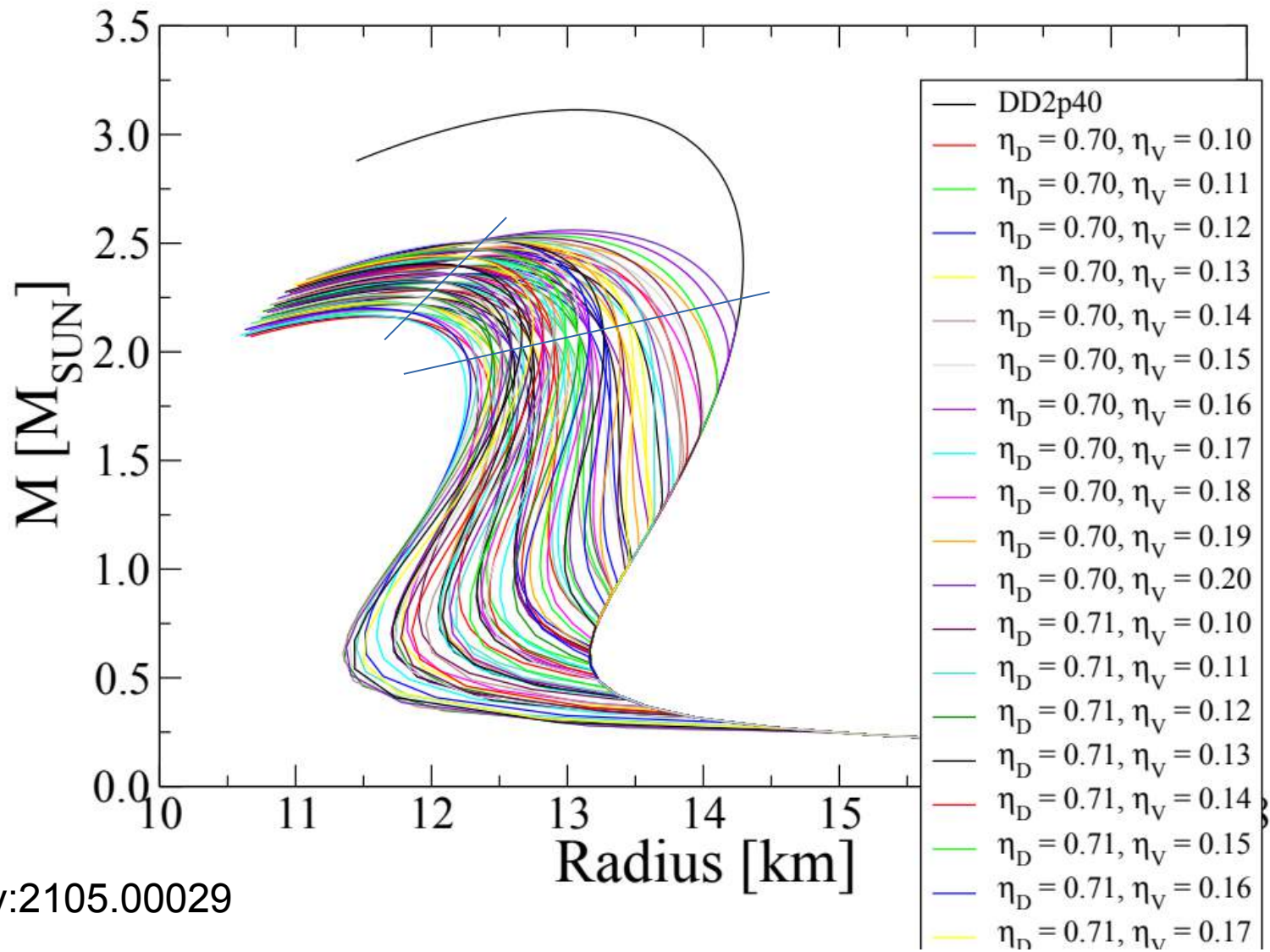
Constant sound speed (CSS) vs. nonlocal NJL model

“Trains” of special points, when η_D and η_V are varied systematically (grid)



Constant sound speed (CSS) vs. nonlocal NJL model

“Trains” of special points, when η_D and η_V are varied systematically (grid)



Old paradigm: hybrid stars smaller and lighter

Works on **Special Point** with M. Cierniak: 2012.15785 & 2009.12353; EPJ ST 229, 3663 (2020)

Dense quark plasma in color
superconducting phase: nINJL mode

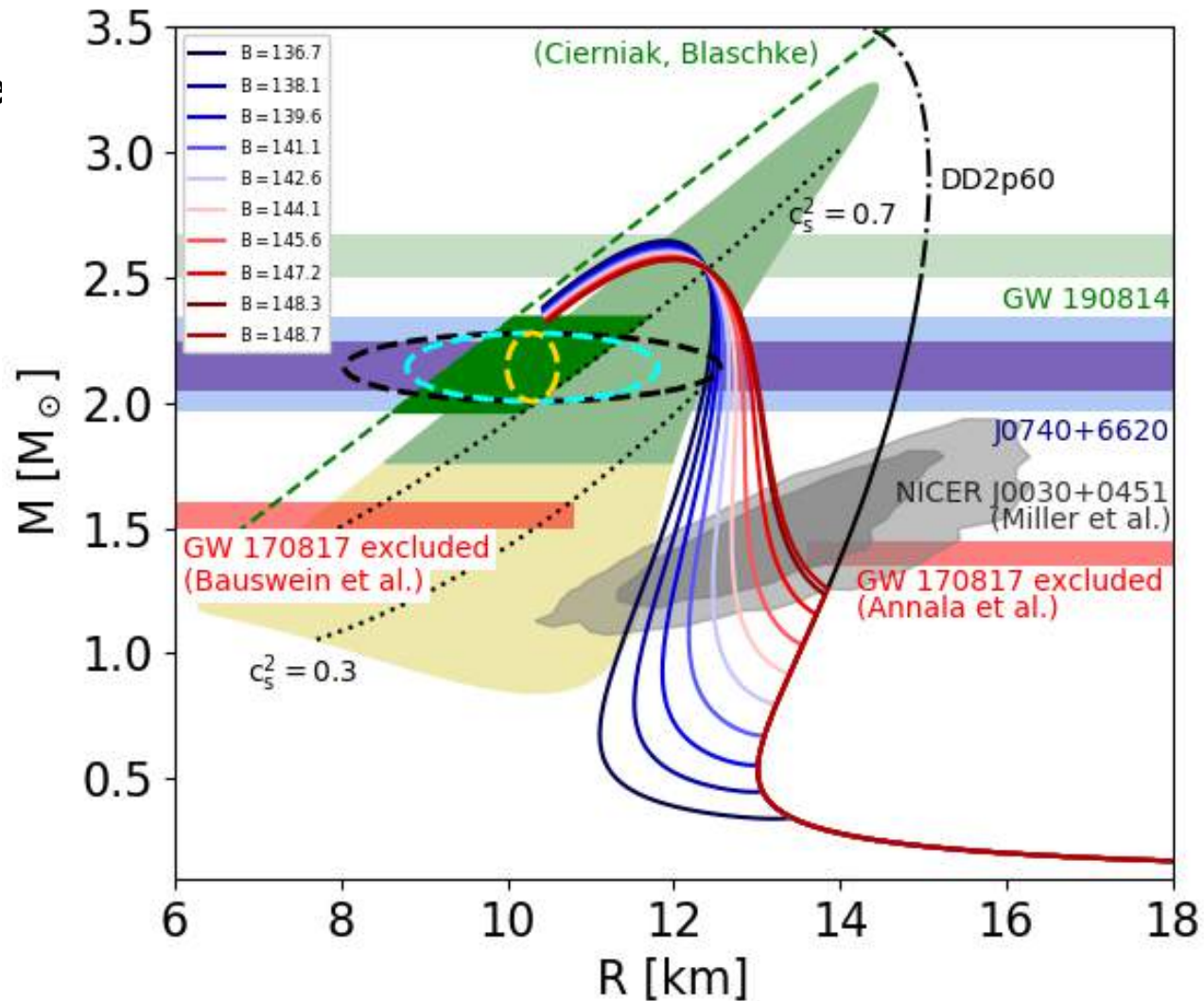
Constant-speed-of-sound (CSS)
Equation of state (EoS)

$$p(\mu) = A(\mu/\mu_0)^{1+c_s^{-2}} - B,$$

$$p = c_s^2 \varepsilon - (1 + c_s^2)B$$

Perfect mapping nINJL \rightarrow CSS,
Antic et al., arxiv:2105.00029

Maxwell construction with
(1st order phase transition)
Relativistic Density Functional
EoS "DD2pxy" by S. Typel
With density-dependent coupling
And excluded volume $v=x.y \text{ fm}^3$



2.6 M_{sun} object can be a hybrid neutron star! With early onset of deconfinement and twins!
NICER radius measurement on PSR J0740+6620 will put constraints on this too!

New paradigm: hybrid stars larger and heavier

Work based on **Special Point location** with M. Cierniak, in preparation

Dense quark plasma in color
superconducting phase: nINJL model

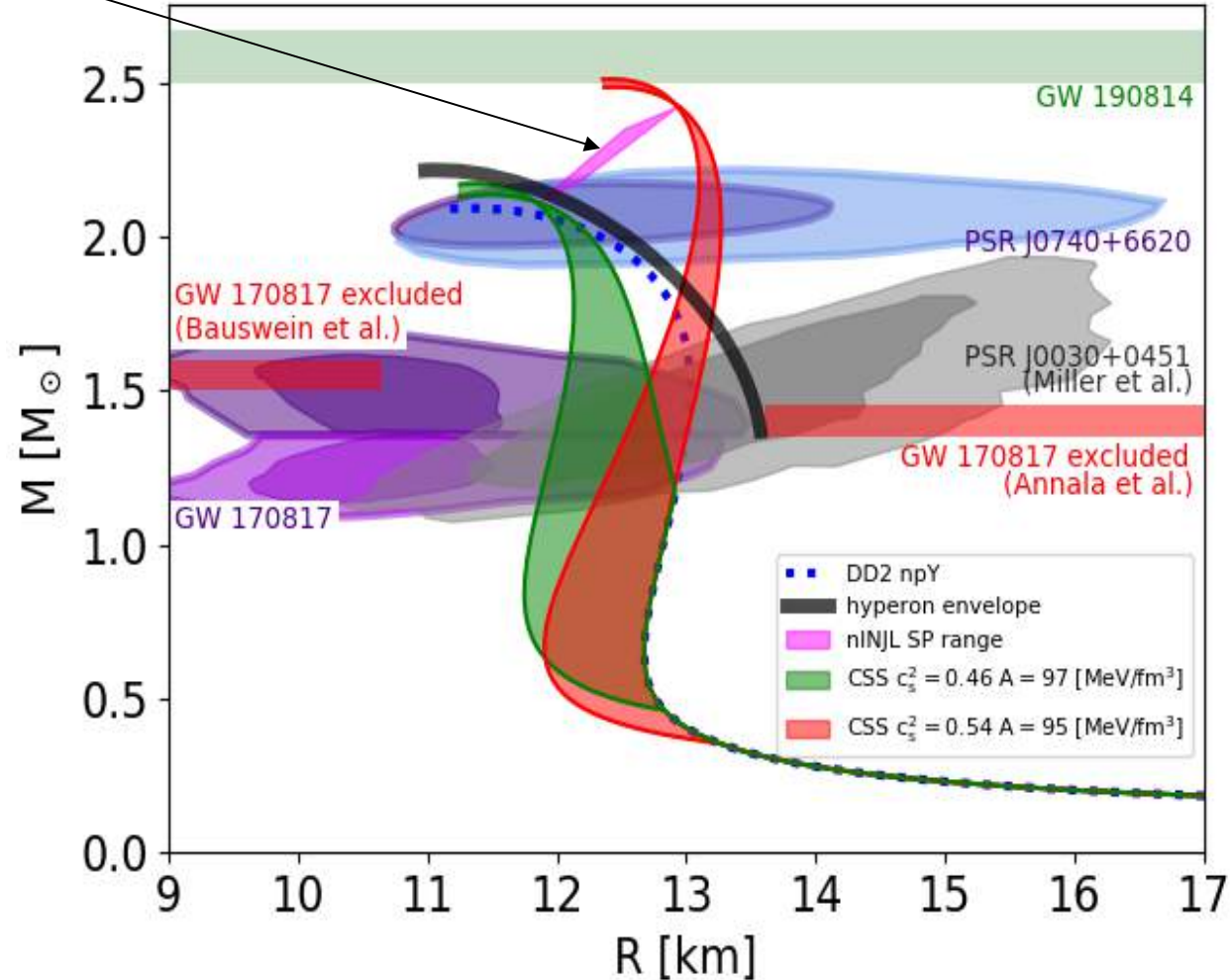
Constant-speed-of-sound (CSS)
Equation of state (EoS)

$$p(\mu) = A(\mu/\mu_0)^{1+c_s^{-2}} - B,$$

$$p = c_s^2 \varepsilon - (1 + c_s^2)B$$

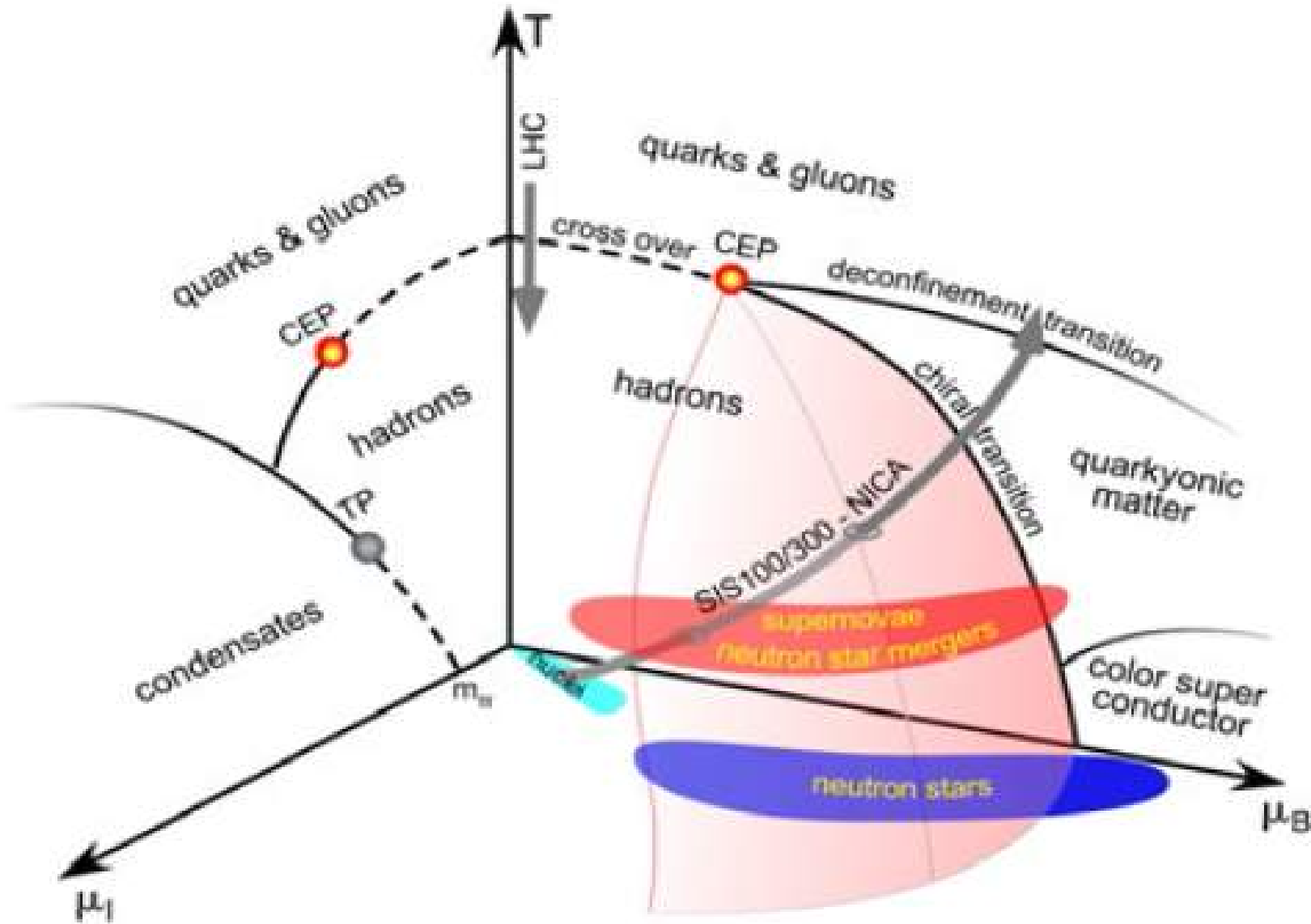
Perfect mapping nINJL \rightarrow CSS,
Antic et al., arxiv:2105.00029

Maxwell construction with
(1st order phase transition)
Relativistic Density Functional
EoS “DD2-Y-T” by S. Typel
With density-dependent coupling



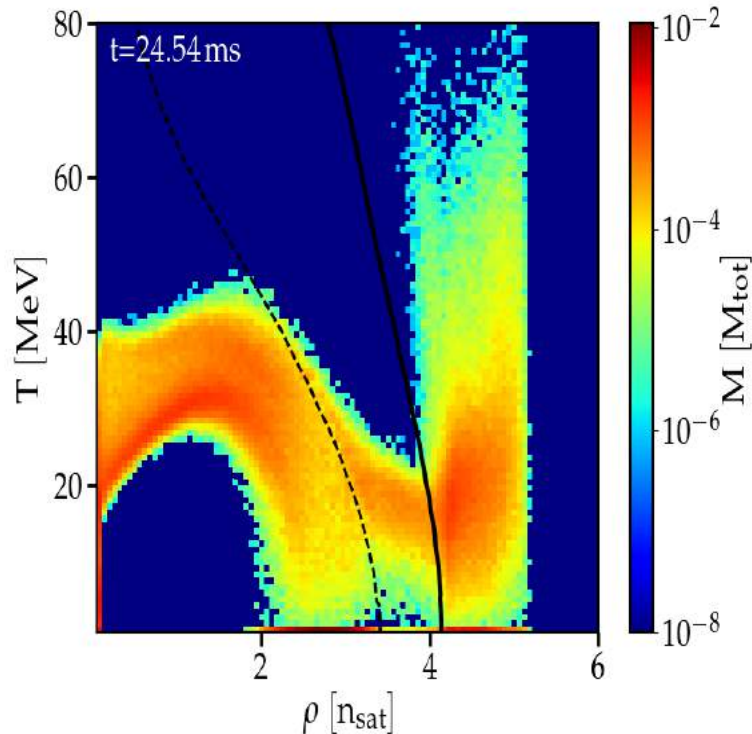
2.5 M_{sun} object can be a hybrid neutron star! With early onset of deconfinement!
NICER radius measurement on PSR J0740+6620 best described by hybrid stars!

CEP in the QCD phase diagram: HIC vs. Astrophysics



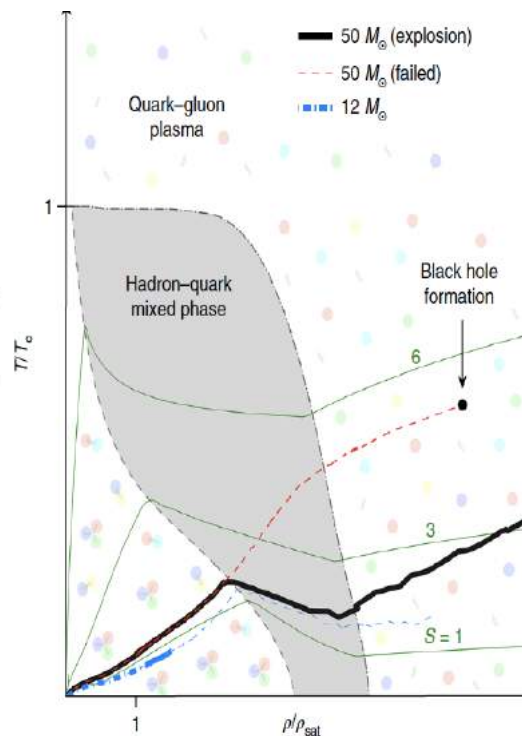
Population of the QCD Phase Diagram

Binary NS merger,
1.35+1.35 M_{sun}



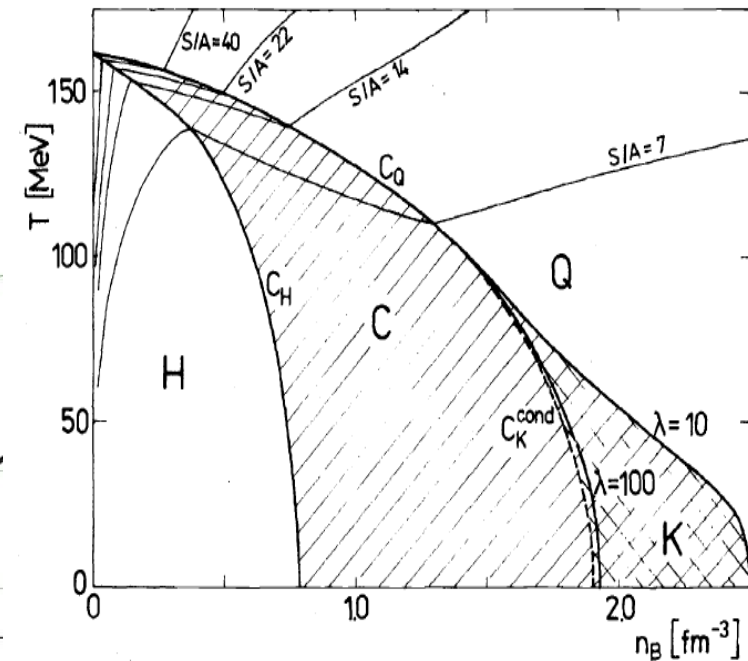
S. Blacker, A. Bauswein et al.,
PRD 102 (2020) 123023
arXiv:2006.03789

SN explosion,
Progenitor 50 M_{sun}



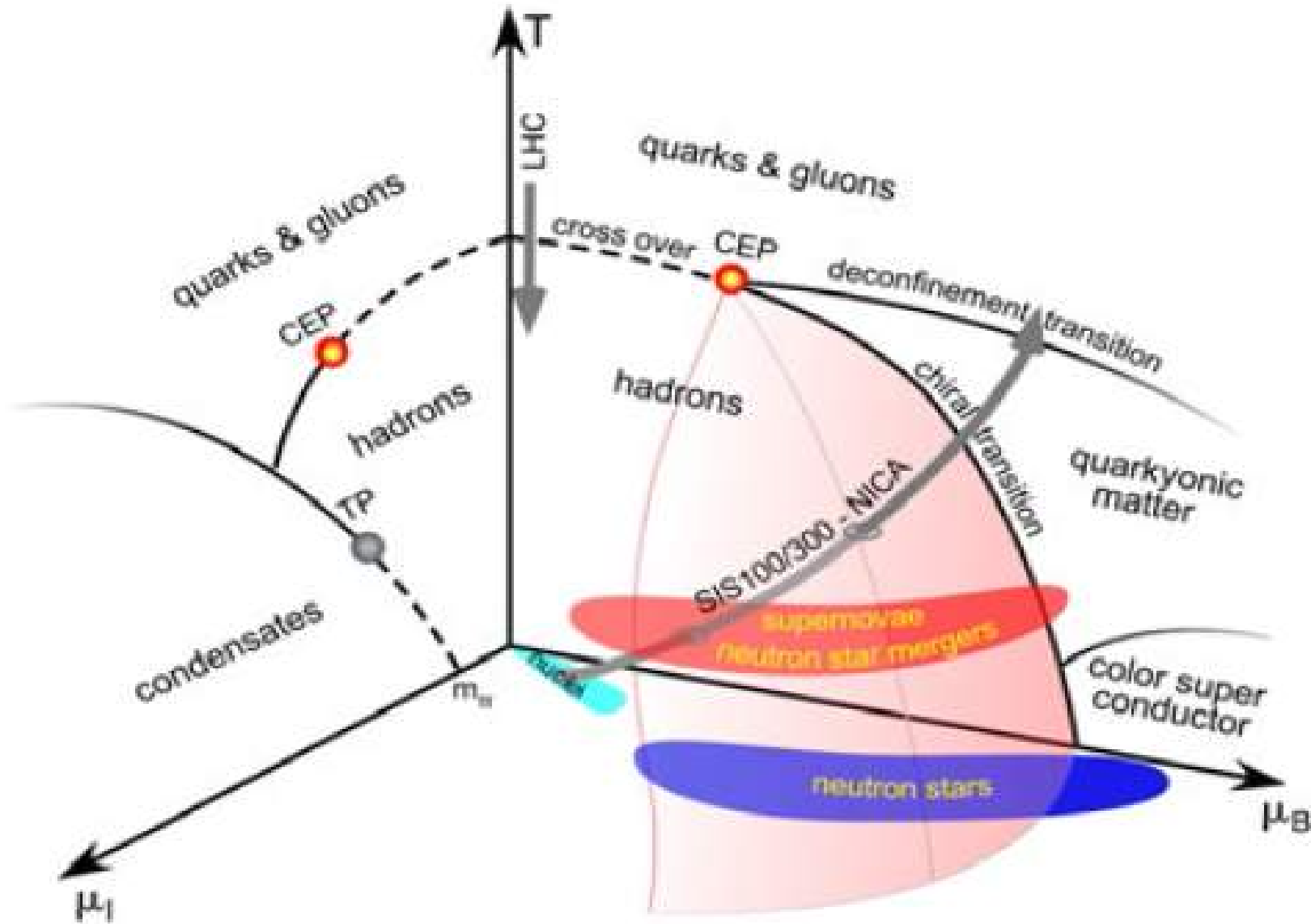
T. Fischer et al.,
Nat. Astron. 2 (2018) 980
arXiv:1712.08788

Ultrarelativistic HIC,
 \sqrt{s} [GeV]=16, 10, 7, 4



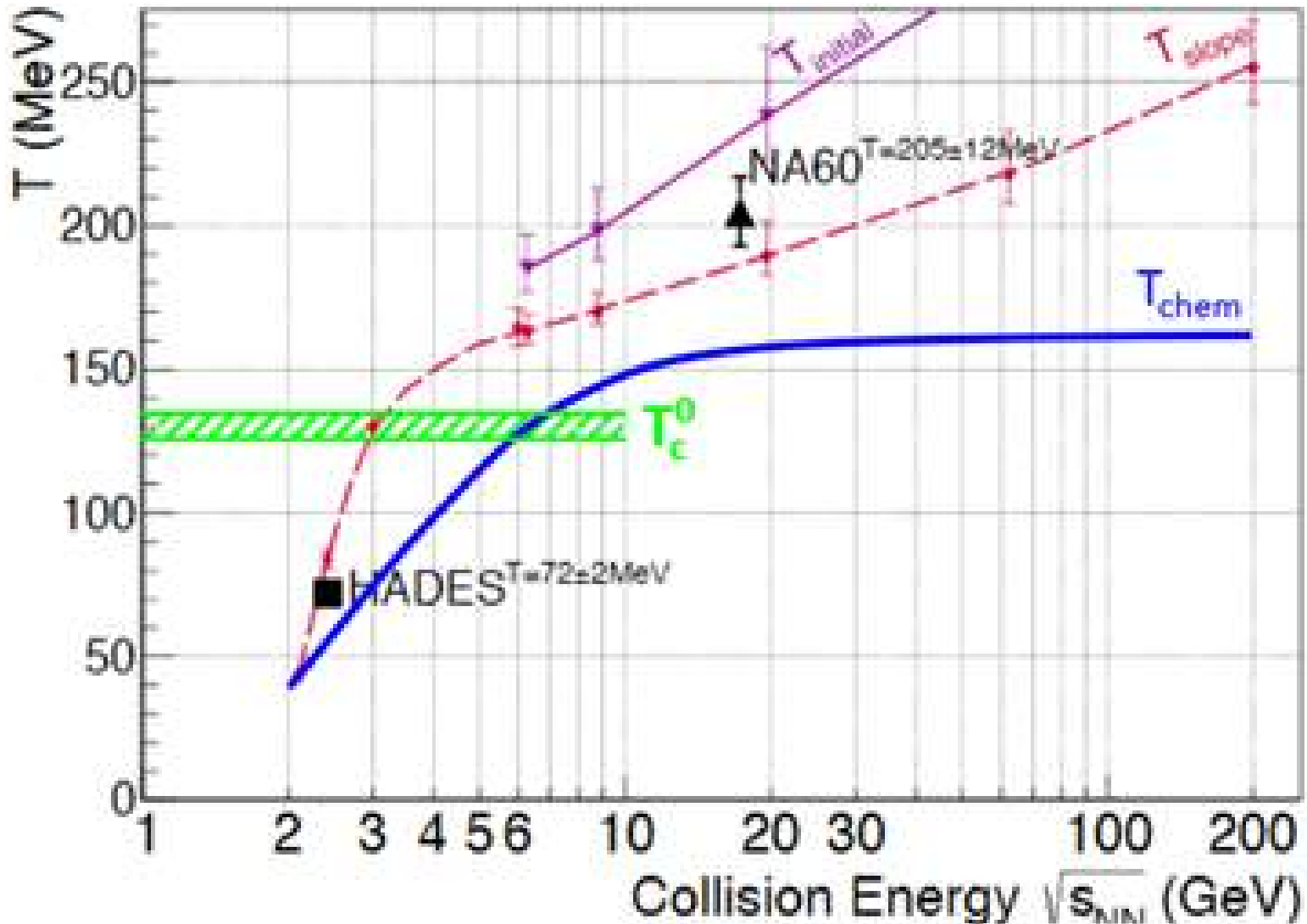
H.W. Barz, B. Friman et al.,
PRD 40 (1989) 157
GSI Preprint, GSI-89-13

CEP in the QCD phase diagram: HIC vs. Astrophysics

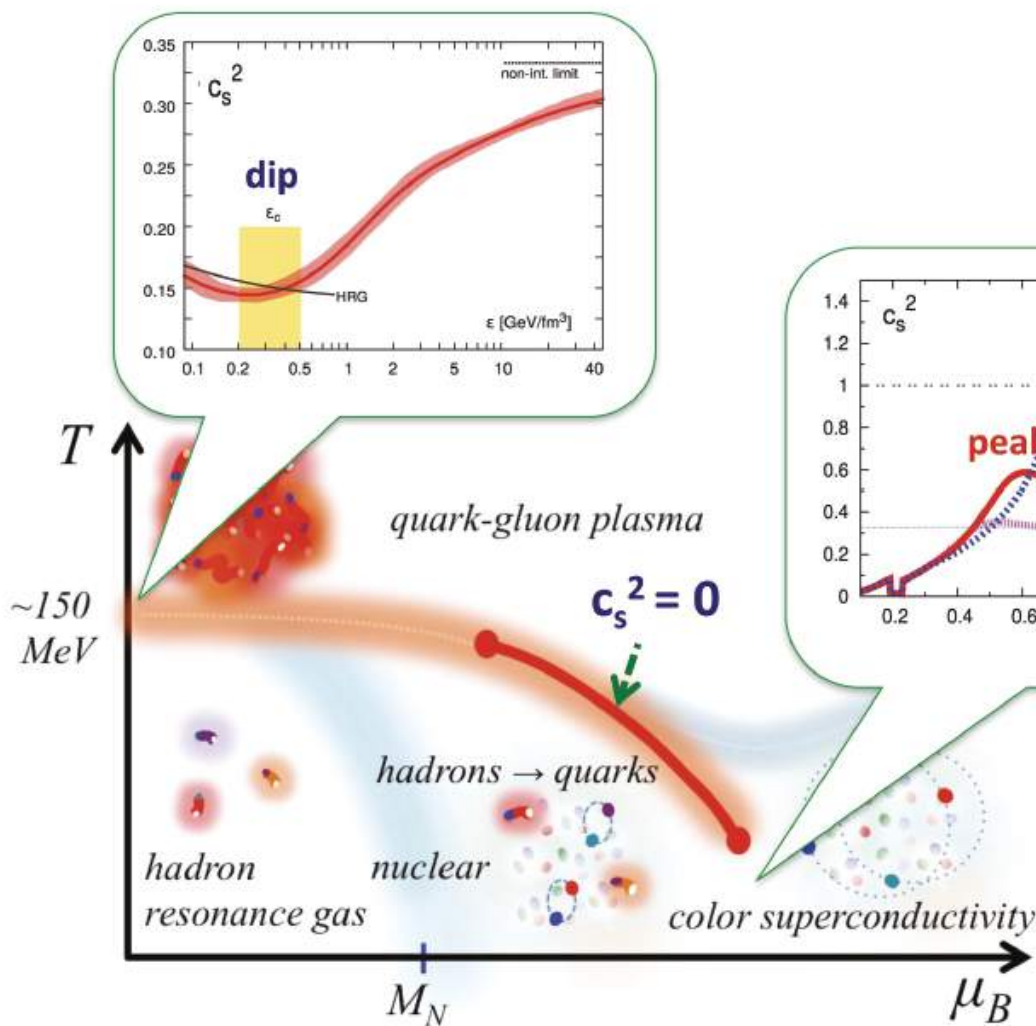


CEP in the QCD phase diagram: HIC vs. Astrophysics

NICA experiments (BM @N, MPD)



2nd CEP in QCD phase diagram: Quark-Hadron Continuity?



Gluons \leftrightarrow Vector mesons
 Quarks \leftrightarrow Baryons
 Goldstones \leftrightarrow Pseudoscalar mesons

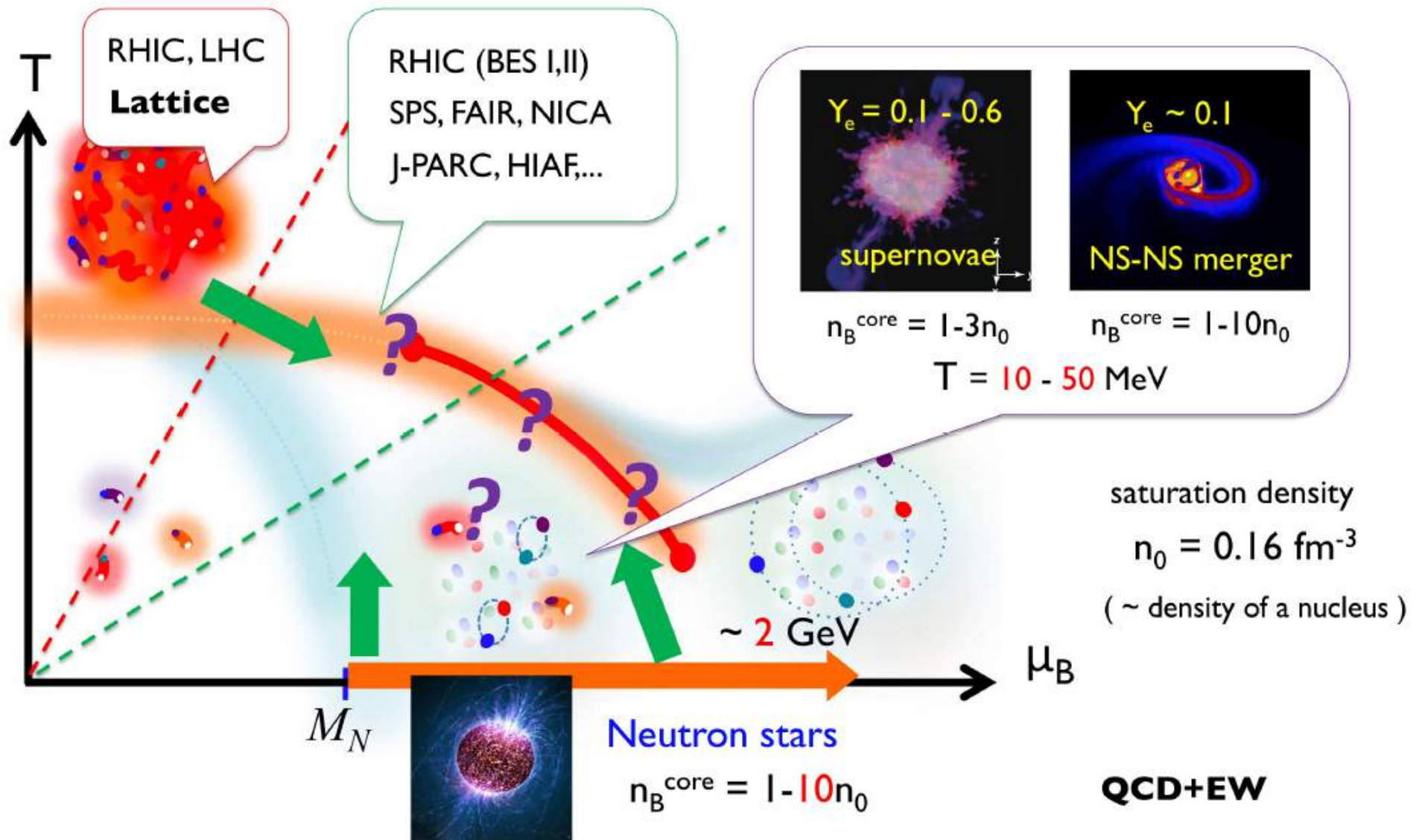
From: T. Kojo,
 "QCD equations of state in
 quark-hadron continuity",
 Universe 4 (2018) 42

T. Schaefer & F. Wilczek, Phys. Rev. Lett. 82 (1999) 3956

C. Wetterich, Phys. Lett. B 462 (1999) 164

T. Hatsuda, M. Tachibana, T. Yamamoto & G. Baym, Phys. Rev. Lett. 97 (2006) 122001

2nd or no CEP in QCD phase diagram: Crossover all over ?



Conclusions

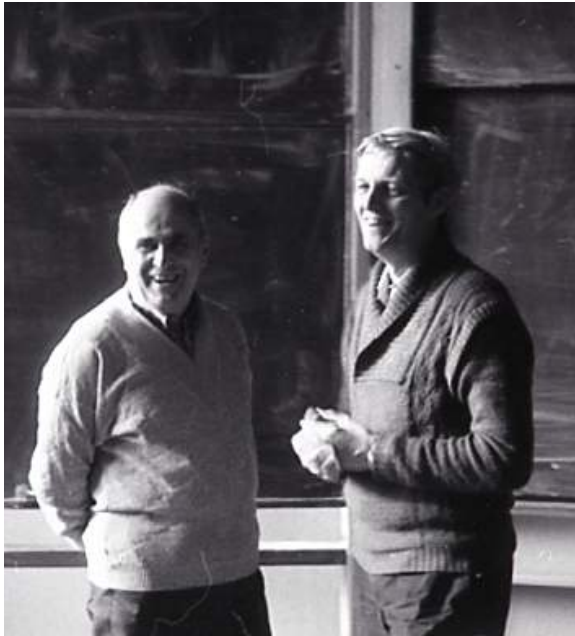
- First observations of binary mergers open new possibilities to constrain properties of the quark-gluon plasma at low temperatures and high baryon densities. Hybrid EoS are developed that allow to estimate quark plasma parameters in hypermassive (proto-) neutron stars
- GW170817: narrow window of small radii at $1.4 M_{\text{sun}}$ (Capano et al.: $10.4 < R_{1.4}[\text{km}] < 11.9$) strongly suggests an early onset of deconfinement with a critical density $n_c < 2 n_0$ and an onset mass $M_{\text{onset}} < 1.0 M_{\text{sun}}$ [Blaschke & Cierniak: 2012.15785]
- GW190814: the lighter object in the extremely asymmetric merger with its $2.6 M_{\text{sun}}$ can be either the heaviest neutron star or the lightest black hole. The central baryon density in such high-mass hybrid stars reaches $5.3 n_0$. Our EoS allows it to be a hybrid star ...
- NICER radius measurement on PSR J0740+6620 triggers a new paradigm: NS with $M > 2M_{\text{sun}}$ should have a deconfined quark matter core when $R_{2.0} > 13 \text{ km}$!

Such a result is similar to the “two families” scenario of Drago & Pagliara, PRD 102 (2020); For the baryon density at the center of a star with $2.1 M_{\text{sun}}$ we find $n < 5 n_0$, $n_0 = 0.15 \text{ fm}^{-3}$.

- Consequences for supernova simulations: A new lower limit for onset of deconfinement?
- Consequences for merger simulations: Check the GW signal for deconfinement !
- Good news for entering a color superconducting quark matter phase at NICA (BMAN, MPD)

In memoriam: Edvard Vartanovich Chubaryan (05.05.1936 – 17.09.2021)

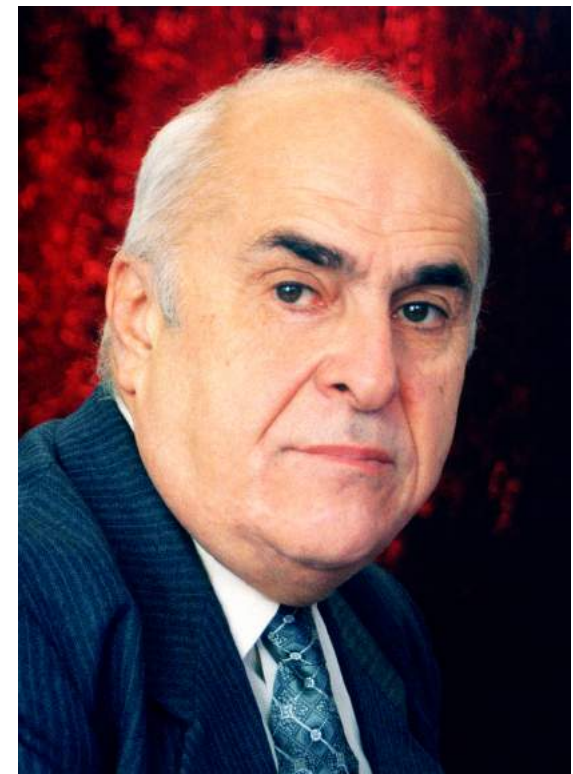
Edvard Vartanovich was instrumental in developing and maintaining the scientific contacts between Yerevan State University and University of Rostock within the Cooperation agreement that has been concluded in 1986.



With Gerd Röpke in front of the blackboard. Small lecture hall of the Institute of Physics at Rostock Univ. (1990).



Walking at the beach promenade around Hotel "Neptun" in Warnemünde with my daughter Anne-Sophie (1990).



1936 born in Spitak
1964 PhD at YSU

1968 publication of first axially symmetric solutions in general relativity together with David M. Sedrakyan; independent of the solutions by Hartle and Thorne obtained at the same time

1972 Doctor of Sciences
1985 – 2000 and 2006 – 2013
Head of the chair for Theoretical Physics.

Worked on Thermodynamics of degenerate superdense matter in the Theory of heavenly bodies

2021 died in Yerevan

Astron. Astrophys. 357, 968–976 (2000)

A joint publication

ASTRONOMY
AND
ASTROPHYSICS

Deconfinement transition in rotating compact stars

E. Chubarian¹, H. Grigorian^{1,2}, G. Poghosyan¹, and D. Blaschke²

¹ Yerevan State University, Department of Physics, Alex Manoogian Str. 1, 375025 Yerevan, Armenia

² Universität Rostock, Fachbereich Physik, Universitätsplatz 1, 18051 Rostock, Germany (blaschke@darss.mpg.uni-rostock.de)

Received 1 February 2000 / Accepted 15 February 2000